# An Assessment of Methane Hydrate Recovery and Processing at Hydrate Ridge

FSc 503

**Pismaniye Aslanlari**

George Alexander
Masoud Almarri
Esra Eren
Elise Fox
Deepa Narayanan

With Contributions from:
Pradeep Indrakanti
Ramya Venkataraman

# Table of Contents

# List of Tables

# List of Figures

## Introduction

Vast quantities of methane have been discovered in the form of solid gas-hydrates in sediments and sedimentary rocks within ~2000m of the earth's surface. These reserves are located in polar and deep-water regions that may just help supplement the current fossil fuel reserves. (Kvenvolden, K. A., 1995).

Gas hydrates are crystalline solids consisting of gas molecules, mostly methane, each surrounded by a cage of water molecules. They look very much like water ice. Methane hydrates are stable in ocean floor sediments at water depths greater than 300 meters (Kvenvolden, K. A., 1988).

Gas hydrates were first discovered in laboratories in the early 1800s but it took almost 150 years to find them in nature. (Link, D. D., 2003) The formation of hydrates depends on:

- Presence of sufficient amounts of water
- Presence of hydrate former
- Appropriate temperature and pressure conditions

In a methane hydrate reservoir, free gas, water, ice and other components like ethane, propane, hydrogen sulfide and carbon dioxide can be found at different temperatures, pressures and depth values. Two and three phase equilibria curves are used to determine the correlation between phases. Those equilibrium conditions may depend on the amount of components. Additionally, if there are very small or large amounts of water in the system, there won't be hydrate formation although the conditions are in the hydrate region. (http://www.telusplanet.net/public/jcarroll/HYDR.HTM)

The maximum amount of methane gas that can occur in methane hydrate is fixed by the clathrate geometry at $CH_4$ $5.75H_2O$ (Kvenvolden K.A., 1995) but mostly the formula of solid methane hydrate is assumed as $CH_4.6H_2O$. Under standard conditions, the volume of methane hydrate will be 164 times less than volume of gas methane. Laboratory experiments have shown that it is sometimes hard to reach even 30% of this theoretical amount. (Link, D.D. et al., 2003)

Until now all endeavors to successfully recover and use this resource have been carried out on pilot plants and on small scales. It may be impractical because most of the production techniques are conceptual and have not been on a large scale. According to Kvenvolden and Lorensen's research, natural hydrates have been found in seventy seven places around the world (Kvenvolden K.A., 1995). The characteristics of methane hydrate deposits are different in different areas, because of the difference in origin, biogenic or thermogenic, their crystalline structure, temperature and pressure conditions necessary for their formation, and their association with different geological formations.

## Geology

A potentially significant source of methane hydrate lies eighty kilometers off the coast of Oregon, USA. The hydrate is situated upon an accretionary ridge owing to the tectonics within the Cascadia basin. The upper Miocene crust of the Juan de Fuca plate is being subducted beneath the North American plate at 40-45 mm/yr, directed at N69$^{o}$E at the Cascadia subduction zone (Figure 1) [Trehu and Fleuh, 2001].

### Methane Transport & Structure

Methane produced from underthrust sediments may be transported as dissolved gas and/or free gas. Hydrate accumulations develop according to this transport of methane. Stratigraphic accumulations develop from low fluid flux settings. These accumulations typically result in lower hydrate concentrations as dispersed pore crystals, nodules, and plate crystals [Milkov, 2002]. Structural accumulations develop from high fluid flux regions leading to higher hydrate pore saturations [Milkov, 2002].

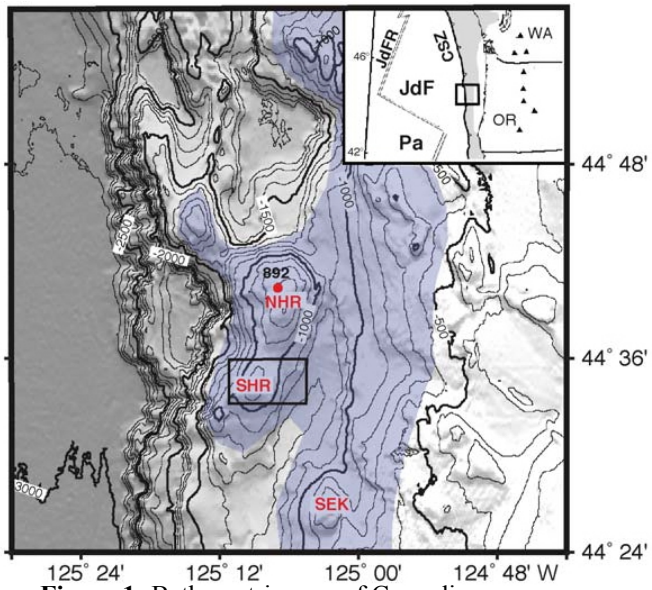


**Figure 1**: Bathymetric map of Cascadia accretionary prism [Trehu et al., 2004].

Specific to the Hydrate Ridge are horizons B and B´, coarse grained layers and horizon A, an ash-rich layer. Horizon A acts as a conduit that spans Hydrate Ridge and transports fluids from the accretionary prism to the southern summit [Trehu et al., 2003]. This horizon has resulted in structural hydrate accumulations at South Hydrate Ridge that approach 40% pore saturation in close proximity to the seafloor, providing a potentially economical resource [Trehu et al., 2004].

### Hydrate Ridge Characterization

A seismic reflection survey from the ODP Leg 146 in 1989 revealed a bottom-simulating reflector (BSR), which is indicative of methane hydrates, beneath the middle and lower slope of the Cascadia accretionary prism [Trehu et al., 2003]. BSRs mimic the seafloor as they produce a negative polarity seismic reflection, signifying a decrease in the acoustic impedance (seismic velocity x density) [MacKay et al., 1994; Trehu et al., 2003]. The presence of free gas overlain by methane hydrates has been detected from a difference in the seismic velocities. Vertical Seismic Profiling (VSP) and borehole measurements have shown that the free gas extends to considerable depths beneath the BSR, possibly upto several hundred meters [Travert et al., 2001]. This figure is difficult to estimate as there is no phase boundary to constrain depth [Travert et al., 2001], but estimates for site 1248 and 1249 are provided in Table 1.

**Table 1 : Free Gas Estimates [Trehu et al., 2004].**

| Region | Concentration, mM | Free gas zone thickness,m | Billion, $m^3$ |
|---|---|---|---|
| 1248, 1249 | 80 | 300 | 1.11 |

Although free gas estimates remain vague, estimation techniques for methane hydrates yield firmer results. Integrating data from pressure core samplers, chloride pore water concentrations, infrared thermal scans of cores, and resistivity-at-bit provide quantitative estimates (Table 2) of hydrate-bound methane [Trehu et al., 2004].

**Table 2: Methane Estimates From Methane Hydrates [Trehu et al., 2004].**

| Region | Area, $km^2$ | Average % Saturation | BSR, mbsf | Estimated Volume of methane x $10^8$ $m^3$ | | Estimated Volume of methane x $10^8$ $m^3$ /$km^2$ |
|---|---|---|---|---|---|---|
| 1248, 1249 | 0.32 | 10 | 115 | 3.68 | | 11.5 |
| 1245, 1247, 1248 | 9.65 | 2 | 129 | 24.90 | | 2.58 |
| 1246, 1244 | 5.9 | 1 to 8 | 119 | 7.02 | 56.17 | 1.19 |
| 1252, Slope basin | 18.4 | 1 | 185 | .36 | | .02 |
| 1251 | 18.28 | 5 to 8 | 185 | 1.69 | 2.70 | 0.09 |
| Total | 35.99 | | | 37.65 | 87.81 | |

## Stability & Transport

Methane hydrates form within sediment pore volumes altering the permeability and the elastic properties of the sediments and potentially, seafloor stability. Historic evidence suggests a connection between instability and the presence of hydrate [Clennel et al., 1999]. The production of methane hydrate adds to the complexity of safety. Questions of cementation, occlusion of pores, packing deformation, drained versus undrained behavior, subsidence and finally slope failure need to be understood qualitatively on a grain to grain scale, prior to production.

In-situ hydraulic conductivity for site 1244 was determined by analysis of pressure core sediment samples. In calculating the permeability from hydraulic conductivity pure water was assumed. With this assumption, the permeability was determined to be between $1.5 \times 10^{-14}$ to $1.3 \times 10^{-15} m^2$ [Tan et al., 2003]. Production models for the summit region of Hydrate Ridge utilize these values from site 1244 due to similarities in the lithology and site characteristics as well as a general lack of site specific data to calculate permeabilities on the summit. The production capabilities are intrinsically tied to the permeability, which also links the slope stability.

Revolving around cementation, the lithology plays a large role in the production potential and stability of a site. The southern summit of Hydrate Ridge consists of clay and silty clay particles [Trehu and Fleuh, 2001]. Similar to ice, hydrate in finer sediments, such as clay, form hydrate lenses, pellets, or sheets similar to permafrost environments [Clennel et al., 1999]. A stern layer remains in liquid form and is partially responsible for the lack of cementation.

Depending on hydrate pore volume saturation and the overburden stress, the clay grains may or may not be deformed (figure 2, b. and c.). It is assumed that as the radius of curvature of the water decreases with hydrate formation, approaching the grain to grain contacts, the pressure required to displace the water will overcome the overburden stress and deformation will occur prior to complete pore occlusion [Clennel et al., 1999]. Therefore the overburden stress has secondary control on the formation of methane hydrate, only after methane requirements are fulfilled for massive formation (Figure 2). Quantification of stability is further complicated by two distinct regions within the gas hydrate stability zone due to hydrostatic and lithostatic pressure profiles.

Figure 3 illustrates that at 19 meters below the seafloor (mbsf) lithostatic pressures provide impending grain deformation. From 19 mbsf to the bottom of the hydrate stability zone, overburden stresses overcome the hydrate pressure and act to confine the hydrate. Above 19 mbsf the internal hydrate pressure is greater than the overburden stress and the hydrate formation is able to separate the

grains. Due to reduced overburden stresses, 30-40% hydrate pore saturations occur in the sediment nearer the sea floor followed by concentrations between 2 and 8% as the BSR is approached [Trehu et al., 2004]. The characteristics of Leg 204 sites 1249 and 1250 demonstrate promise for methane accumulation and potential recovery. Broader evaluation of the Cascadia Basin and site specific lithological evaluation will prove valuable for recovery operations as grain characteristics influence not only the stability but also the hydrate reserves.

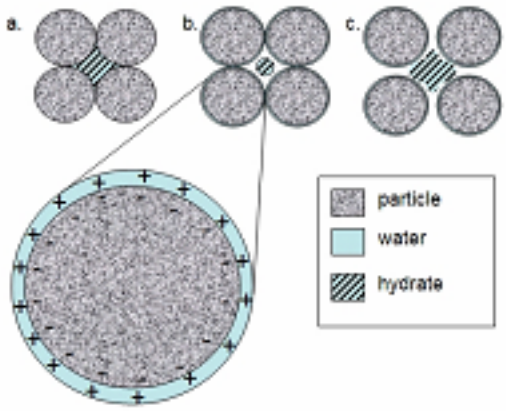


**Figure 2: Hydrate-grain interactions for pore growth with sand and clay**

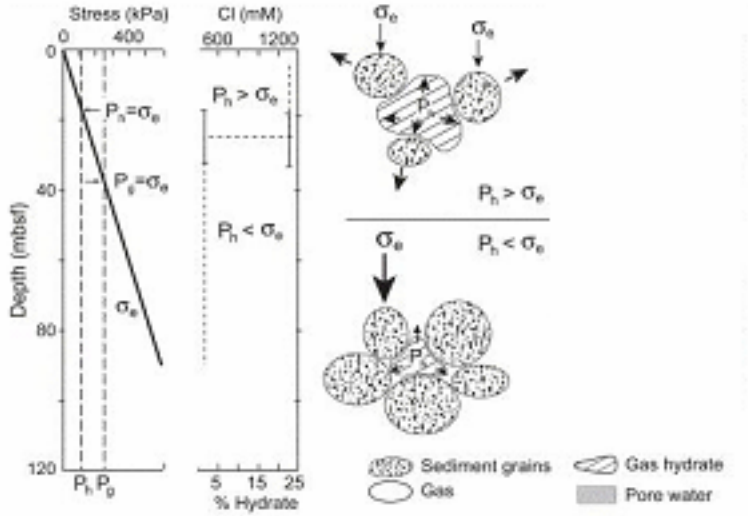


**Figure 3: Schematic representation of depth on grain deformation [Trehu et al., 2004]**

# 3 Recovery of Hydrates

Hydrates are known to occur at temperatures less than 295 K and pressures greater than 3000 KPa. The hydrates at Oregon are taken to be of cubic structure I (sI) which predominates in the Earth's natural environments (Sloan E. D. Jr 2003) and the dissociation of these hydrates occurs as –

$$CH_4.6H_2O_{(s)} \rightarrow CH_{4(g)} + 6H_2O_{(l)}$$

$\Delta H_{Enthalpy}$ = 10 ~ 20 Kcal / mol of gas dissociated(Holder G. D. 1982)
This reaction requires an external energy source to propagate along the right hand side(Trehu A.M. 2004). There are three techniques currently under study to recover gas from methane hydrates (Collett T.S. 1998)

1) Inhibitor injection
2) Depressurization
3) Thermal stimulation

They influence the stability of hydrates in a manner as shown in the figure –

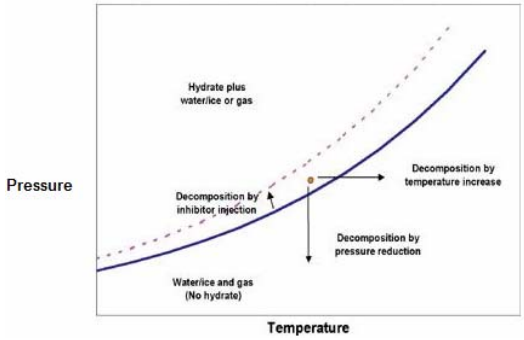


**Figure 4: Effect of depressurization, temperature stimulation and inhibitors on the hydrate stability curve (Pooladi-Darvish M. 2004).**

## Inhibition of Hydrates

In most offshore applications, hydrate formation is controlled by injection of a thermodynamic hydrate inhibitor. Inhibition injection is carried out via the use of one of the inhibitors listed below at a given pressure, which will reduce the temperature at which hydrates form.
Common inhibitors can be alcohols (methanol), glycols (ethylene glycol) and ionic salts. Several types of inhibitors have been tested for positive results but it has been determined that glycols and alcohols are the most successful ones. The principle by which alcohols, glycols and salts inhibit hydrates is the same. However, salts have some corrosion problems and also due to low vapor pressures, they can not vaporize. In the model reviewed here, methanol (MeOH) and ethylene glycol (EG) are examined and compared in many ways such as chemical structure, physical properties, cost analysis, safety concentration limits, environmental considerations and dehydration capacities.

Beside temperature and pressure conditions, composition and sufficient amount of inhibitors must be determined. The inhibitor must be at or below its water dew point (i.e. must be water-saturated). In addition, dehydration can be used as an alternative.

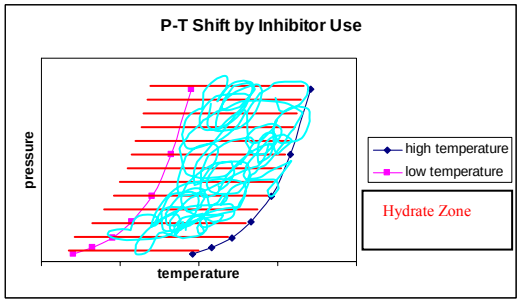


In Figure 4, the temperature decreases at specific pressures and facilitates hydrate dissociation. While red colored area implies hydrate zone, after temperature depression, free gas will form and hydrate zone will shift to the left to lower the temperature side. While MeOH has a vapor pressure (16.8) and indefinite water solubility, EG's solubility is limited by 10g/100ml and has lower vapor pressure (0.06). Methanol can easily shift to the gas phase due to the low vapor pressure.

**Figure 5: P-T Shift showing hydrate dissociation due to inhibitor use**

The assumptions considered in the model are:

1) Inhibition rate is a function of temperature and pressure but the effect of pressure on inhibition rate

is slight, and subsequently it will be neglected.

2) Inhibitor injection rate taken as constant.

In order to find the required amount of inhibitor needed to produce a unit amount of methane, first temperature depression amount and then dissociation rate with respect to weight percent of concentration of inhibitors will be calculated. The Hammerschmidt equation is used to calculate the temperature depression in the hydrate dissociation via presence of inhibitors [Sloan, Jr., E.D., 1994]. In that equation a temperature decrease depends on the weight percent of inhibitor and molecular weight of inhibitors. However, this equation is limited to inhibitor concentration of less than 20 wt% and above 250K temperatures. So, another equation used is found from the study of Sira et al. in 1990 which $\Delta T$ and X are the parameters for temperature and wt% inhibitor in solution, respectively.

Inhibition effects depend on both temperature and pressure but pressure only slightly affects inhibition of hydrates so it is neglected in the modeling of inhibition. Again, it is assumed that there is continuous inhibitor injection to the system [Lederhos et al, 1996].

Many aspects need to be considered during injection of inhibitors into gas hydrates like the shift in the equilibrium curve, dissociation rate, properties of inhibitors, etc. The actual amount of inhibitor required for producing a mole of methane from gas hydrates and how much it costs and dissociation rates of inhibitors are shown in Table 3.

**Table 3: Calculated values in production model by chemical inhibitor injection**

| | Methanol | Ethylene Glycol |
|---|---|---|
| Methane Production Rate | 3 MMSCF/D | 3 MMSCF/D |
| Injection Rate | $3.9 \times 10^5$ kg/day | $4.1 \times 10^5$ kg/day |
| Inhibitor Unit Price | $ 0.84/ gallon | $ 4.75 / gallon |
| Total Cost | $125,000/day | ~$ 500,000/day |
| Concentration in Water, % | 35 % | 22 % |

## Comparison of Methane Hydrate and Ethylene Glycol

Technology used with EG inhibitor provides a lower cost, safer concentration limits, and a more environmentally attractive alternative to methanol for hydrate prevention in offshore gas lines. Although it is a general consideration, calculated values in the inhibitor injection model supports this judgment. Ethylene glycol is recovered with a higher efficiency than MeOH. Therefore, without recovery facilities, large makeup volumes of methanol required to inhibit the high volume of gas would represent an extremely high operating cost. The unit price of methanol and ethylene glycol is found as $0.84 (www.methanex.com) and $4.75 (www.lakehurts.navy.mil) per gallon, respectively. At first sight, it may seem methanol use as an inhibitor costs less but recovery and recycle costs, which is an operating cost, exceeds the lower unit price of methanol.

Furthermore, methanol poses greater safety risks in handling and storage than EG. Flash points of methanol and EG are 52°F and 232°F, respectively. So methanol can be easily ignited. Also, as environmental considerations TLV TWA values of very toxic ethylene glycol and methanol are comparably higher as 50 ppm and 200 ppm, respectively. Those values are much higher than the usual limits so it requires extra safety conditions. (based on the article http://www.gasprocessors.com/GlobalDocuments/E1Nov_01.pdf)

## Depressurization

(Moridis G. J. 2003) classified hydrate reservoirs based on the geological and reservoir conditions. The Oregon site under consideration fit the description for a class 1 reservoir. Software that can simulate multi-component, multiphase fluid and heat flow and transport in the subsurface called TOUGH2 was used in conjunction with the EOSHYDR2 module for solving the coupled equations of mass and heat balance. Based on the calculations depressurization was shown to be the most promising technique for the class 1 type of reservoirs. Depressurization has also been quoted by many researchers as the most economically viable option (Makogon Y.F. 1997; Pooladi-Darvish M. 2004). Following this work, the depressurization technique was studied in this section.

There are three important mechanisms involved in the depressurization of the gas hydrates- kinetics of dissociation, heat transfer including conduction and convection and flow of fluids like gas and water.

A lot of work has been done to obtain a complete 3 Dimensional model in a porous media which would simulate the exact conditions of a reservoir with regard to all the mechanisms involved but so far researchers have been able to arrive at answers only with certain assumptions.

(Makogon Y.F. 1997) developed both radial and Cartesian models using Darcy's law, mass balance equations for hydrates, gas and water and heat transfer equations including conduction, convection and a change in temperature due to throttling and adiabatic coefficients. But when the analytical solutions were obtained, conduction terms were ignored. The rate of decomposition, the rate of production of gas and water, were calculated with consideration to permeability variation.

(Holder G. D. 1982) arrived at a numerical solution for a three dimensional simulation by considering gas flow and ignoring water flow. Conduction terms were incorporated into the model but the convection terms were ignored. The rate of hydrate dissociation at the surface was determined by the dissociation enthalpy obtained from the energy balance equations.

The analytical model developed by Hong et al in 2003 accounts for the intrinsic decomposition of the hydrate that results in a change in temperature along with heat transfer and flow of fluids (Hong H. 2003). Hong acknowledged the importance of each of the important mechanisms for dissociation – kinetics, heat transfer and fluid flow and developed a model wherein each of the mechanism is independent of the other.

(Moridis G. J. 2004) used the TOUGH2 model with the EOSHYDR2 module to arrive at one of the most comprehensive models, which included conduction, convection, flow of gas and water, mass and heat balance.

The radial analytical model developed with decomposition kinetics by (Goel N. 2001) completely ignores the change in reservoir temperature due to enthalpy of dissociation of hydrates and fluid flow. The model assumes a single-phase fluid flow where the dissociated water does not affect the flow, which is not quite true as water reduce the fluid transport within the system. This model does not permit modeling of a constant withdrawal rate.

A one dimensional model with heat transfer effects including conduction and convection is considered with a numerical solution that was generated by (Ahmadi G. 2004) and it was mentioned that conductive heat flux plays a dominant role in supplying the heat for dissociation. This model arrives at the conclusion that the well pressure controls the rate of gas production and that conduction also plays a dominant role. It also highlights that the reservoir temperature affects the temperature gradient in the region near the front. This model gives the mass and heat balance at the dissociation front.

A one dimensional, three phase fluid flow model with the effects of conduction and convection is considered to arrive at an analytical solution (Tsypkin G.G. 2000). The mass and energy conservation

laws were used and natural gas was assumed to be a perfect gas. The kinetics was ignored. The conclusion of this work was that formation of ice leads to reduction in gas permeability and this affects the gas production volume. The work considers dissociation of gas hydrates co-existing with water and dissociation of hydrates in low temperatures.

After a study of the different models and keeping in mind the complex nature of the problem, a simple tank model proposed by (Khataniar S. 2002) was followed to understand the basic nature of the problem and to understand which of the reservoir parameters has the maximum influence on the production rate and time of well abandonment.

The reservoir is considered to be of tank geometry. The output of the well includes gas from both the free gas zone that lies beneath the hydrates and from the dissociation of hydrates. With time, as gas is withdrawn from the reservoir, the pressure decreases, the equilibrium pressure shifts so as to re-establish equilibrium. The dissociation is considered analogous to ice melting – it occurs along the front instead of the entire volume [Ahmadi 2004]

## Model

## Model

Assumptions

1) The reservoir behaves as a tank model with one centrally located production well
2) The reservoir is considered as homogenous and isotropic with a hydrate zone and an underlying free gas zone
3) Depressurization is considered as the driving force for hydrate dissociation
4) There is no intermediate phase in the hydrate zone. There are only three phases – hydrate (solid), natural gas (gas) and water (liquid)
5) The effect of water released is considered in the mass balance
6) The well is assumed to be homogenous in all rock properties i.e., there is no variation with different locations on the type of material and is isotropic with respect to permeability
7) Connate water and rock expansion are negligible
8) Instantaneous equilibrium in terms of pressure and temperature is achieved throughout the gas zone
9) No external water drive exists – the reservoir behaves as a closed system with no-flow boundaries and all the water produced is assumed to be from dissociation of hydrates i.e., there is no free water in the reservoir other than that coming from hydrate dissociation
10) Heat transfer from surrounding zones are neglected
~~11) Permeability is assumed to be constant and considers single phase flow values~~

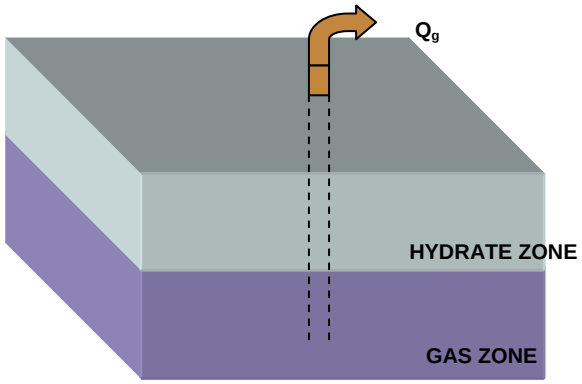

**Figure 6: Reservoir Kinetic model (Khataniar S. 2002)**

Nomenclature

| Nomenclature | | Value |
|---|---|---|
| A | Surface area of hydrate | 1500 $m^2$ |
| *$B_g$ | Gas formation volume factor | 0.02 |
| *$B_{gH}$ | Hydrate formation volume factor | |
| *$B_w$ | Water formation volume factor | 1 |
| $G_{fi}$ | Initial free gas in place | 1E9 $m^3$ |
| $G_{Hi}$ | Initial gas hydrate in place | 2.3E6 $m^3$ |
| $G_{Hr}$ | Hydrated gas remaining | |
| $G_p$ | Gas produced | |
| $h_{Hi}$ | Initial hydrate zone thickness | 115m |
| $h_{gi}$ | Initial gas zone thickness | 300m |
| n | Backpressure exponent | 0.5 |
| $P_{He}$ | Hydrate decomposition pressure | 5.47E3 KPa |
| $P_{wf}$ | Well flowing pressure | 1600 KPa |
| K | Effective permeability | 5E-15 $m^2$ |
| $S_{wi}$ | Initial water saturation | 0.15 |
| $\mu_g$ | Viscosity of gas | 1E-8 KPa S |
| $\mu_w$ | Viscosity of water | 1.50E-6 KPa S |
| $W_{eH}$ | Water influx from hydrates | |
| $W_p$ | Water produced | |
| $\Phi$ | Porosity | 0.2 |

* - Formation volume factor – Volume of fluids change when they are brought from reservoir conditions to standard atmospheric conditions. This factor accounts for that change so that all results are in terms of STP conditions.

Equations

1 $m^3$ hydrate = 164 $m^3$ gas
1 mole of hydrate = 1 mole of gas + 6.15 moles of water

At time = t,
The change in volume of hydrate from time t=0 to t=t is

$$\Delta V_H = (G_{Hi} - G_{Hr})B_{gH} = A\phi(1 - S_{wi})\Delta h_H$$

The change in volume of water caused by dissociation of hydrates is

$$\Delta V_w = (W_P - W_{eH})B_w = A\phi(S_{wi} - S_w)h_g$$

The change in the volume of free gas is

$$\Delta V_g = G_{fi}(B_{gi} - B_g) + (G_p - G_{eH})B_g$$

For a closed bounded reservoir, the net change in volume should be 0

$$(G_{Hi} - G_{Hr})B_{gH} + (W_P - W_{eH})B_w + G_{fi}(B_{gi} - B_g) + (G_p - G_{eH})B_g = 0 \quad \text{---- (1)}$$

The molar rate of dissociation is taken as mentioned in (Kim H. C. 1987)

$$\frac{dG_{eH}}{dt} = K_o A\phi e^{\frac{-E}{RT}}(P_{He} - P) \quad \text{---- (2)}$$

where $K_o = 2.2838*10^{17}$ scf gas/acre-psi-day
E / R = 16950 $^0$R = 9416.666 K

Differentiating the equation with respect to time, the rate of change of hydrate zone thickness as a result of hydrate decomposition is given as

$$\frac{dh_H}{dt} = K_o A\phi e^{\frac{-E}{RT}} \frac{(P_{He} - P)B_{gH}}{(1 - S_{wi})} \quad \text{---- (3)}$$

The standard backpressure equation used to model gas inflow to the production well

$$Q_g = \frac{dGp}{dt} = C\left(P^2 - P_{wf}{}^2\right) \quad \text{---- (4)}$$

Where C is the deliverability constant of the well and is usually determined analytically in terms of reservoir properties accounts for reservoir rock and fluid properties, flow geometry and transient effects.

The water production rate is given by

$$Q_w = \frac{k_w \mu_g B_g}{k_g \mu_w B_w} Q_g \quad \text{---- (5)}$$

The rate of water influx from hydrate decomposition is

$$W_{eH} = 8.33*10^{-4} G_{eH}$$

Differentiating equation (1) with respect to time and then pressure and substituting the final free gas volume

$$\frac{dP}{dt} = \frac{\left[ B_g Q_g + \left\{ 1 + \frac{k_w \mu_g}{k_g \mu_w} \right\} - \left\{ B_g - B_{gH} + 8.33 * 10^{-4} B_w \right\} \frac{d(G_{eH})}{dt} \right]}{\left[ A\phi(1 - S_w) h_g \frac{1}{B_g} \frac{d(B_g)}{dP} \right]} \quad \text{---- (6)}$$

## Depressurization Results & Conclusions

Steps to arrive at graphs and results -

Step 1 - Assuming that the effect of conduction can be neglected because it is smaller by many orders than the effect of convection generated by movement of fluids caused by the low pressure near the well, Figure 7 is derived from this understanding that at this surface, pressure is continuous and is related to temperature by the correlation of phase equilibrium between free gas and hydrate as –

$$\log P_D = a(T_D - T_0) + b(T_D - T_0)^2 + c \quad \text{----(7)}$$

Where a = 0.0342
b = 0.0005
c = 6.8404

From this graph and from the information that the temperature of the methane hydrate in the Oregon site is 4 – 10 $^{o}$C, which is averaged to ~ 6 $^{o}$C, the value of the hydrate equilibrium pressure is found to be = 5400 KPa

Step 2 - The next step is to determine the values of $B_g$ for the different pressures the reservoir reaches as it gets depleted. These values are calculated by using the equations;

$$PV = nRT$$

$$V_{reservoir} = \frac{P_{STP} * V_{STP} * T_{reservoir}}{T_{STP} * P_{reservoir}}$$

$$B_g = \frac{V_{reservoir}}{V_{STP}}$$

Figure 8 is plotted to verify the trend of variation of $B_g$ with reservoir instantaneous pressures. The reservoir is assumed to be gradually brought down to atmospheric conditions. But since atmospheric conditions are attainable only in an ideal situation, a well flowing pressure that is slightly higher is assumed at 1600 KPa. This does not account for the hydrostatic head.

Step 3 - In equation 4, the pressure term is squared to account for the pressure dependence of the fluid properties. The value of the backpressure exponent is assumed to be 0.5 to account for turbulence of flow. The deliverability constant accounts for reservoir rock and fluid properties, flow geometry and transient effects. Initially, the value of the deliverability constant is assumed the same as that of the author (Khataniar S. 2002). This value is specific to each reservoir and is found analytically when well tests are conducted. Reducing the pressure in steps and using equation 4 the values of rate of gas flow is calculated.

Step 4 - The volume of water produced is calculated by using equation 5 and from the assumption that there is no free water in the reservoir other than that coming from hydrate dissociation.
Using equation 2, the molar rate of dissociation is calculated.

Step 5 - Finally, using equation 6, the dp/dt values are calculated and since the dp values are known, the time values can be calculated.

Step 6 - Using the time values, graph $Q_g$ vs. t is plotted as shown in Figure 9. After the initial set of calculations, the value of C is varied and different $Q_g$ vs. time is plotted. The area under each of these curves is taken to find the lifetime yield of the reservoir. Now the C value is found and fixed at the value in which the reservoir gives the maximum yield. This C value was found to be 0.05 $m^3$/s/KPa.

Step 7 - $Q_w$ vs. time is plotted as shown in Figure 10, the percentage of hydrate dissociated vs time is plotted as Figure 11, the percentage of hydrate contribution to the total gas production vs time is calculated as Figure 12.

Step 8 - To test what factors influence the production of gas the most, different E/R values, different deliverability constants, different initial reservoir pressure conditions are assumed and percentage contribution from hydrate vs t graphs are plotted as in Figures 13, 9, and 12.

The deviation from conventional reservoirs found in this model is that, in a conventional reservoir, the slower the production rate, the longer it takes to recover the maximum amount of hydrocarbons, and the greater the yield from the reservoir. In this reservoir, the slower the production rate and longer is takes to recover the maximum amount, the lesser the yield.

Figure 12 shows that there is very little hydrate dissociated, this is possibly due to the rate at which the depressurization occurs – more than 90% of the pressure drop occurs within the first 12 hours of commencement of the well production.

Unlike the results of the model adapted from the (Khataniar S. 2002) paper, the Figure 9 generated here doesn't have a hydrate dissociation state because of the high rates of production that we are assuming. The reservoir modeled here is not getting a chance to attain a pressure equilibrium. This is also the reason why the percentage contribution from hydrates is extremely low because there is not sufficient time for the dissociation process to progress.

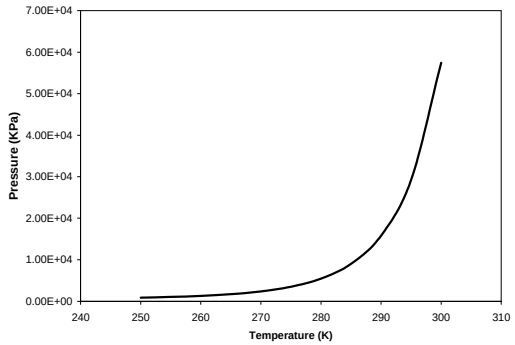


**Figure 7: Stability Graph of Hydrates (Pd vs Td)**

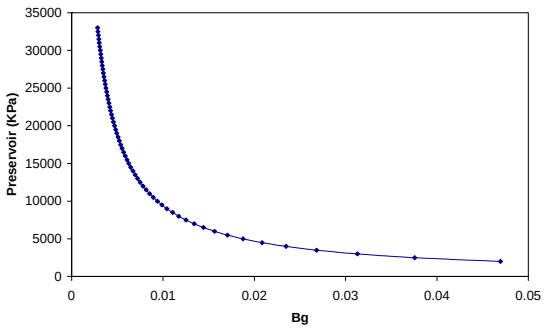


**Figure 8: Reservoir vs Bg**

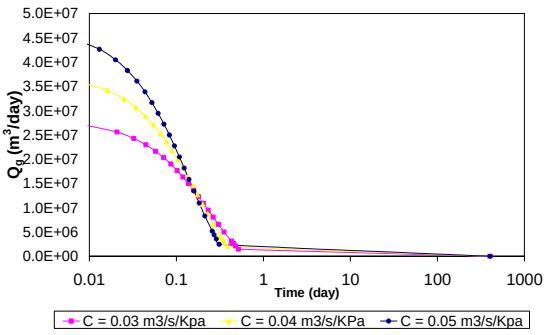


**Figure 9: Effect of Deliverability on Gas Prod. Rate**

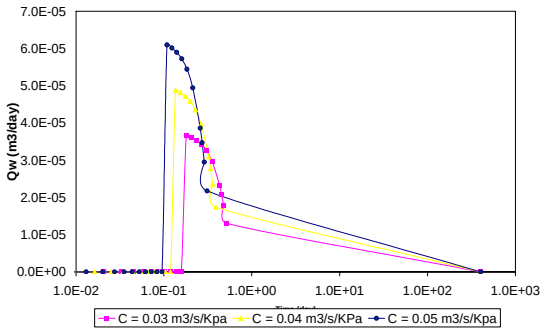


**Figure 10: Effect of Deliverability on Water Prod. Rate**

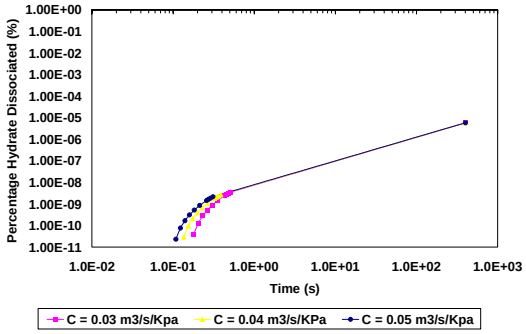


**Figure 11: Effect of Deliverability on Hydrate Decomposition**

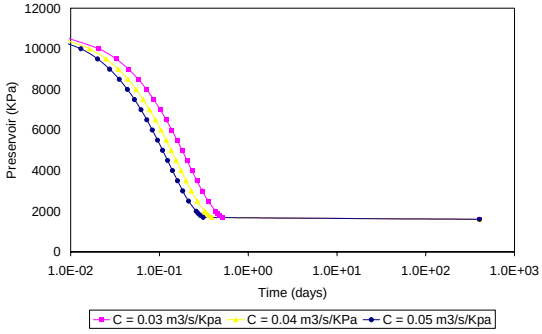


**Figure 12: Pressure Change wrt Time**

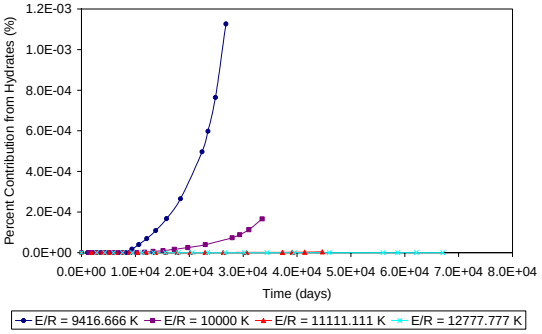


**Figure 13: Effect of Activation on Cont. of Hydrates to Cont. of Hydrates to Gas Prod.**

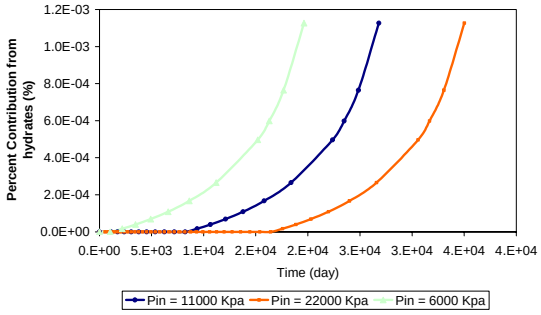


**Figure 14: Effect of Initial Reservoir Pressure on Cont. of Hydrates to Gas Prod.**

## Hydrate Removal/Mining Techniques

The first concern is that of obtaining drilling rights from the US government. Oregon owns the coastal waters from the coastline to 3 miles out in the ocean beyond which the Outer Continental Shelf (OCS) begins. Since the proposed site is nearly 60 miles out in the ocean, it is in the OCS. The OCS permit exists only in Alaska at present. The OCS lands act requires the Department of Interior (DOI) to prepare a 5 year program that specifies size, timing and location of the areas to be assessed for Federal Offshore leasing. The DOI makes sure that the US government gets a fair share for leasing the land and take steps to protect the environment. Lease sales are held on an area-wide basis and the highest bidder is awarded the lease. To date there has been no interest expressed in the Oregon coast. (DOI 2004), (EPA 2004)

The next step is to drill a wildcat or exploratory well. Normally this is done to check for hydrocarbons. This step will also be used to test the practical applicability of this technique to withdraw hydrates from the sea. A mobile offshore drilling unit (MODU) is used for this purpose. MODUs are of two types, bottom supported units and floating units. Bottom supported units are jack-ups and submersibles types. The floating units are of the two types - drill ships and semi-submersibles. (Baker 1998)

The issue at hand is that the hydrates are located at depths below the sea level but the rock material above the hydrate is neither as hard nor is it as thick as those above conventional oil and natural gas wells. Since the hydrates are not in well-defined spaces bound by hard cap rock, there is a chance of slope failure and this can be a considerable safety concern, a floating drilling unit is the best technique to use in this situation. Drill ships, which are mobile and can be moved around to different sites seems to be the best option since we have relatively low concentration of hydrocarbons, spread over an area. Drill ships can have two derricks and can drill in two nearby spots at the same time. Drill ships are also the best for the kind of depths (~ 800m) the hydrates are located below the sea level. The weather conditions show that the seas are relatively calm and will not cause severe turbulence issues for the ship.

Once the drilling, casing and cementing is complete, tests have to be run to see if the well should be completed. The simplest method of these is to test the cuttings the drilling mud carries. Well logging is the most widely used evaluation technique. Measure of how the formations respond to electric current or natural and induced radioactive attributes of rocks, speed with which sound travels through a formation is carried out. Once the well has been tested for hydrocarbons, it has to be completed to start production. A perforating gun is lowered into the well, and using shaped charges, perforations are made through the casing and cement. Usually the hydrocarbons are not permitted to flow though the casing or liner. A piece of tubing with a small diameter is placed inside the cased well through which the oil and gas flow out. The tubing terminates on the top at a collection of valves and fittings called a Christmas tree. This configuration permits the operator to control the amount of production or shut the well completely. Flow can also be directed through alternate surface lines as required using this configuration (Baker 1994).

## Future Considerations

The assumption in this work is that one production well can influence the entire area of site 1249 and 1250 which is around 30 * 30 $m^2$. Though the rule of thumb for oil well is one well per acre, this is not applicable to the Oregon site. This is because the thickness of our reservoir is relatively small and the permeability is extremely low. To mitigate this problem, it may be beneficial to have a network of wells. To economize this operation, from one permanent platform, several directional wells can be drilled to exploit the reservoir completely. Horizontal drilling is a part of directional drilling which may enhance the production from the reservoir, given the shallow depths and wide areas over which the hydrates are spread out. The other issue is that single horizontal wells appear have an advantage over single vertical wells by delaying water upcoming and leading to higher contributions of gas from dissociation to the production gas stream. (Moridis G. J. 2004)

Another tactic that can be applied to enhance production is to thermally stimulate the well. This has to be specially considered because of the assumption made in the above model that the heat of enthalpy required to dissociate the hydrate is provided by the heat flow from the surrounding reservoir

area which serves as an infinite reservoir and initiates heat flow towards the cooled zone (the un-dissociated hydrate zone), providing the necessary energy to further decompose the hydrates (Pooladi-Darvish M. 2004). This would have been case, if the thermal diffusivity of the hydrates had been higher by many orders of magnitude. To provide for this deficit in temperature, one of the techniques is steam injection, but the heat losses in the well bore and reservoir can be severe, especially thinner hydrate zones. The use of brine has a distinct advantage over steam in dissociating hydrates (Kamath V.A. 1991)

A two-well system involving a combination of depressurization at the production well and thermal well at the injection well where hot fluids are injected appear to be better than single vertical system. (Moridis G. J. 2004)

Hydraulic mining is another possibility that can be employed to withdraw hydrates from the Oregon region. The idea is to have a mobile unit that can mine one location, exhaust the reserves and proceed to the next location. (Collett T. S. 1998)

Fracturing as considered in the conventional petroleum and natural gas industry is another possible method of increasing yield from the well. This method may not work around hydrates because there's a chance of all the hot brine injected from the injection well would flow directly to the production well, resulting in very low thermal efficiencies. (McGuire P.L. 1982)

## Transportation

There are many transportation options for natural gas - compressed natural gas (CNG), liquefied natural gas (LNG), pipelines, and gas-to-liquid (GTL) product transportation. Pipelines are generally attractive for short distance from the shore due to the low capital investments. However pipeline transportation requires extensive gas processing which will drive the production costs up, making pipeline transportation unfeasible for low production rates and high moisture containing gases.

LNG transportation requires a very high capital investment and for this reason, should not be considered for the Hydrate Ridge site. Alternatively, CNG provides lower operating costs, but incurs high capital costs due to the transportation vessel. This makes CNG ideal for mid-sized reserves which can produce a large quantity of gas over the reserve lifetime to absorb the capital cost of vessel. CNG is an attractive alternative if natural gas hydrate and GTL transportation proves to be a technical challenge or the production costs become too high. GTL transportation has the lowest capital investment for the processing equipment to produce the liquids, but GTL transportation is uneconomical at this point. If the economics of syn-gas production is lowered, GTL transportation is very attractive and should be considered as the mode of transportation.

Figure 15 illustrates the relationship of annual production rate and distance from the market to the modes of gas transportation. As illustrated, LNG is not a feasible option for short distances or low production rates. The figure presents GTL transportation as feasible for long distances for low production rates, this is because of the high capital cost for the GTL processors and CNG and NGH become more economically feasible at shorter distances. However, this can be argued and CNG for Hydrate Ridge sites is not as economically viable as hydrate shipping. The estimates for the economics used by Gudmundsson assume poor GTL conversions based on previous technologies. GTL technologies are becoming more economical and efficient and should not be ignored. Based on this analysis hydrates, GTL and CNG are the more economical transportation modes with CNG being a fall back if hydrates prove too technically challenging and GTL processes are too costly.

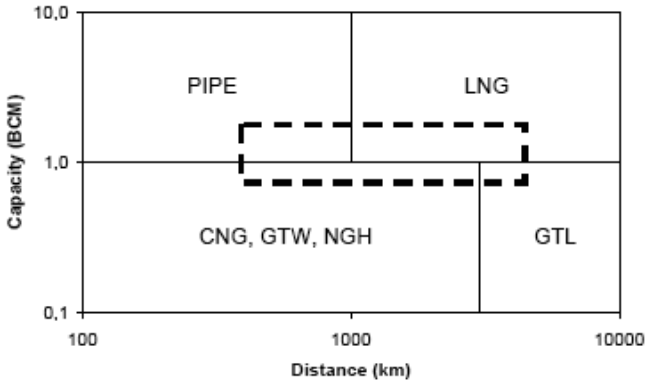


**Figure 15: Relationship of the economics of yearly production rate and distance to the market [Gudmundsson, 2003].**

Overall, hydrate transportation seems to be an attractive transportation mode since extensive gas processing is unnecessary and the main costs are with the production of the hydrates. Since the hydrate production can be performed at milder conditions than LNG, CNG and GTL, hydrate transportation is the most attractive route to delivering the recovered gas to the market place. Based on current research [Giavarini and Maccioni, 2004], it could be feasible to transport methane hydrates at reasonable temperatures and pressures. They found that the best storage conditions were at 0.3 MPa and –4$^{o}$C. Under these conditions there was slow dissociation of the hydrates, with complete dissociation occurring after 40 days showing that methane hydrates may be a feasible commercial transport option over short periods of time. In fact, Mitsui Engineering and Shipbuilding along with Japan's National Maritime Research Institute are currently investigating shipping techniques with methane hydrates [Wolman, 2003]. At this point in time, there needs to be more research and testing to determine if shipping methane hydrates is feasible.

Should hydrate transportation prove not feasible either economically or scientifically, transportation of gas in the form of GTL liquids will be pursued. Since the production rate from the hydrate ridge is so low, it may be necessary to complete processing from the methane hydrate to Fischer-Tropsch fuels on a floating plant at sea, as to be discussed. By shipping these fuels, the costs on natural gas compression or liquefaction are saved. Sea vessels are also readily available for this purpose. In the case that FT fuels are not produced and natural gas is treated at sea, pipelines will be investigated for use.

## Production of Natural Gas from Methane Hydrates

In order to calculate the cost of production of natural gas from methane hydrates, several assumptions have to be made. The assumptions are listed in the table below.

**Table 4: Assumed production values from the Cascadia Ridge hydrate reservoir for production cost determination.**

| | Assumed value |
|---|---|
| Number of Production years | 400 days |
| Amount of gas in reservoir | $1*10^{9}$ scm |
| Amount of recoverable gas | 50% or $5*10^{8}$ scm |
| Production rate for 400 days | $1.3*10^{6}$ scmd |

Using current costs received from the Energy Information Agency [EIA, 2004], a division of the US Department of Energy, an initial assessment of the production cost was made. The operating cost of a 600ft deep 18-slot platform in the Gulf of Mexico, with a maximum production rate of 40Mcfd, was used. This platform, though able to produce at much higher rates than the site in the Cascadia Ridge, is operating at a much shallower depth than this project. The annual operating costs include: labor, payroll overhead, supervision, food, personnel transport, surface equipment, operating supplies, work over, communications, administration, and insurance. The costs for the land lease equipment of a 4000 ft well include: two storage tanks, dehydration, and methanol. No compression or further treatment is included.

**Table 5: Operating costs of natural gas production [EIA, 2004].**

| | Cost /US$ |
|---|---|
| Wellhead price of NG/ 1000cm | $5.36 as of 8/2004 |
| Platform operating costs/ year | $6,795,600 |
| Land lease equipment costs/ year | $29,900 |
| Cascadia Ridge income | $7289.60/day |
| Break even production rate at current cost of operation | 3.17Mcmd |
| Break even NG price at current production | $12.49/1000cm |

## Natural Gas Treatment

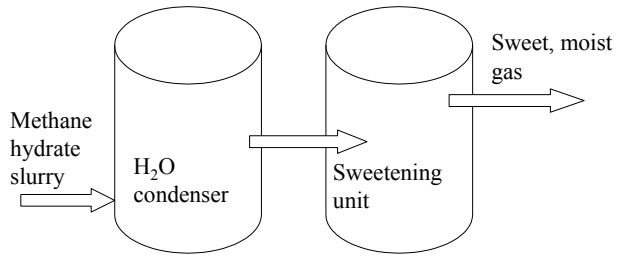


**Figure 16: Proposed processing unit for methane hydrates to be used in GTL technology.**

### Conventional Natural Gas Treatment

Using the natural gas hydrates that are removed via the depressurization model, they may need to undergo processing similar to that of conventional natural gas reservoirs. A conventional natural gas treatment facility goes though three process steps: sweetening, dehydration, and a light oil absorber. After all treatment processes have been completed, the final product is referred to as stripped natural gas. When methane hydrates from the Cascadia ridge are mined and utilized, it is necessary to sweeten the product, because up to 10% $H_2S$ may be present. Significant amounts of $H_2O$ will also be present and need to be removed before compression or liquefaction. There are also nominal amounts of ethane and $CO_2$ also present [Kastner et al., 1995]. Since the natural gas from the methane hydrates will be used for gas-to-liquids technology, removal of $CO_2$ and ethane are not necessary. Easily condensable $H_2O$ will be removed, and the remaining $H_2O$ will aid in the production of synthesis gas.

**Table 6: Sample compositions of methane hydrate core samples.**

| Site | Chemical Composition | Source |
|---|---|---|
| 889 and 892 | ~90% methane, up to 10%$H_2S$, 1 to 600ppm ethane, some $CO_2$ | [Kastner et al., 1995] |
| 1240 | Methane, <29.7mM sulfate, also includes $NH_4^+$, $PO_4^{3-}$ | [Trehu et al., 2003] |

## Dehydration

Dehydration can be costly, yet an important step in natural gas treatment. In this step, water that can cause severe damage to pipelines and valves during freezing is removed. Glycols, such as diethylene glycol, triethylene glycol, and tetraethylene glycol, are commonly used in this process. The numerous oxygen sites on the glycol provide ideal sites for moisture absorption and retention through hydrogen bonding [Schobert, 1990]. The tower used for dehydration may have a countercurrent flow, where the moist gas is injected in the bottom of the tower and the dry gas removed through the top. Other options for dehydration include adsorption, such as using a molecular sieve, gas permeation, and refrigeration.

In the case of methane hydrate use for GTL technology, it is not necessary to remove all the moisture, only the excess amount. A simple condenser, or gas/liquid separator, can easily do this. Since there is a low gas to oil ratio, this separation can occur in 2 stages [Rojey et al., 1997]. The first stage will have pressure from 0.7 to 3.5 MPa, where the dry gas will flow from the top of the condenser and the water will flow to a second condenser that is at 0.16 to 0.6 MPa to remove additional moisture.

## Sweetening

The sweetening process is designed to remove $H_2S$ from the natural gas feed stock. The presence of acidic $H_2S$ in the gas can cause damage to the not only the pipelines and valves, but can also poison catalysts that may be used for reforming of the fuel. Since $H_2S$ is a weak acid, it can easily be absorbed by bases [Schobert, 1990]. Bases such as diethanolamine (DEA) are typically used in this process. Though cost intensive, this is a necessary addition to the stripping process. Research has shown that when 25-30% wt of DEA is used, gases with $H_2S$ concentrations from 9-25% wt can be cleaned [Rojey et al., 1997]. The reactions for DEA with $H_2S$ are listed below.

$$2(CH_3CH_2)_2NH + H_2S \leftrightarrow [(CH_3CH_2)_2NH_2]_2S$$
$$[(CH_3CH_2)_2NH_2]_2S + H_2S \leftrightarrow 2(CH_3CH_2)NH_2HS$$

These amines can also react with $CO_2$ in the feed gas to form carbonates, bicarbonates, and carbamates, whose reactions are listed respectively [Rojey et al., 1997].

$$2(CH_3CH_2)_2NH + CO_2 + H_2O \leftrightarrow [(CH_3CH_2)_2NH_2]_2CO_3$$
$$[(CH_3CH_2)_2NH_2]_2CO_3 + CO_2 + H_2O \leftrightarrow 2(CH_3CH_2)NH_2HS$$
$$2(CH_3CH_2)_2NH + CO_2 \leftrightarrow (CH_3CH_2)_2NCOONH_2(CH_3CH_2)_2$$

The use of physical adsorbents for the sweetening step has several benefits. These benefits include use of high $H_2S$ feed, desired $H_2S/CO_2$ selectivity, high pressures can be used, and they can be used with heavy hydrocarbon concentrations. After the sweetening process, $H_2S$ must be converted to sulfur for environmental concerns. The Claus process, which takes place over a catalyst, reacts $H_2S$ with $SO_2$ as seen below. This process can have up to a 98% sulfur recovery rate when completed in 3 stages [Rojey et al., 1997].

$$2H_2S + SO_2 \leftrightarrow 3S + 2H_2O$$

## Sweetening process for NG Hydrates

The vacuum carbonate process for $H_2S$ removal will be used for the sweetening of the gas produced from methane hydrates. This process is based on a commercial system used by Koppers Co. Two benefits of this process are that the use of a vacuum reduces the water requirement for $H_2S$ treatment and the $H_2S$ is extracted in a sellable quality. This system can tolerate quantities of HCN that may cause damage in other systems.

A flow diagram of the vacuum carbonate system is seen in Figure 17 below. The absorber, dilute $Na_2CO_3$, is packed in a countercurrent absorber tower. The solution is then passed to the actifier tower to be stripped by steam and undergo vacuum regeneration. The solution is removed from the bottom of the actifier tower, cooled, and sent back to the absorber unit. Gases removed from the top of the actifier tower undergo condensation and a vacuum pump system [Kohl and Riesenfeld, 1985]. Heat is required for activation of the system. In this unit, waste heat for the Fisher-Tropsch unit can be passed through heat exchangers to increase the efficiency of the system and generate steam.

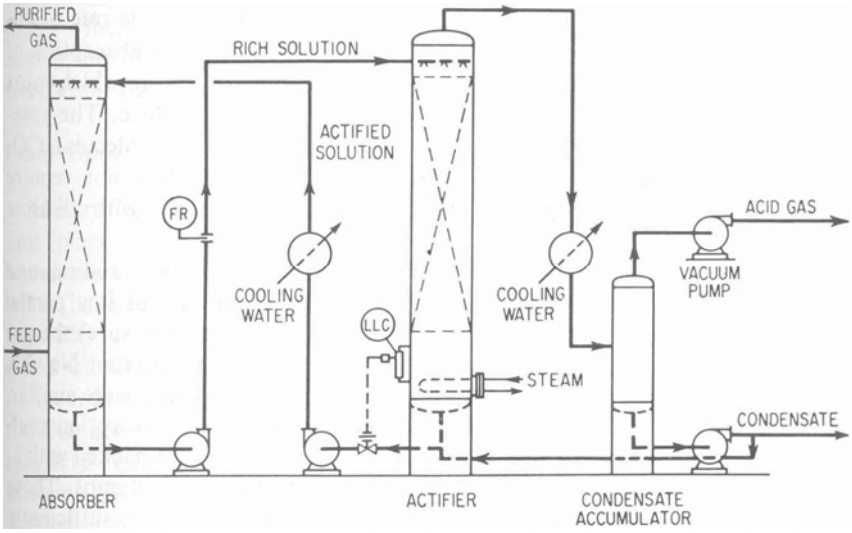


**Figure 17: Flow diagram of the vacuum carbonate process [Kohl and Riesenfeld, 1985].**

The principal reactions in the system for the absorption of $H_2S$ and $CO_2$ are listed below.

$$Na_2CO_3 + H_2S \rightarrow NaHS + NaHCO_3$$
$$Na_2CO_3 + CO_2 + H_2O \rightarrow 2NaHCO_3$$

A side reaction can occur in the presence of air is:

$$2NaHS + 2O_2 \rightarrow Na_2S_2O_3 + H_2O$$

The active material in the tower is considered as alkaline $Na_2CO_3$ for the absorption of $H_2S$. In this unit, the concentration of $CO_2$ is low, so the competitive absorption between the two gases does not become an issue. This sweetening process is often used for coke-oven gases, which may have 250-500 grains $H_2S/100\ ft^3$ and 1.5-3%$CO_2$ [Kohl and Riesenfeld, 1985], and is treated at low pressures.

If naphthalene and ammonia are present in the gas mixture, several problems can occur in the system. Naphthalene can condense in the system causing plugging and ammonia will decrease the efficiency of the process by increasing the solubility of $H_2S$, making it harder to remove from the system. Fortunately, methane from hydrates contains no naphthalene and little ammonia to make these contaminants major issues.

Costs can be estimated from values received from the Koppers Co. for this process [Kohl and Riesenfeld, 1985]. The values in the table below are based on a 55MMscf/day plant using 400 lb/day of $Na_2CO_3$ and 9600 lb/day of steam. Cost savings with and without the heat exchange system are included.

**Table 7: Total daily costs for the vacuum carbonate process [Kohl and Riesenfeld, 1985].**

| Requirement | Unit price | With heat-exchange | Without heat-exchange |
|---|---|---|---|
| Cooling water | $0.015/1000 gal. | $19.10 | $33.80 |
| Electric power | 0.01/kwhr | $78.80 | $16.60 |
| Steam: live | 0.70/1000 lb. | N/A | $122.50 |
| low-pressure | 0.50/1000 lb. | $6.70 | $273.70 |
| $Na_2CO_3$ | 0.02/lb. | $8.00 | $8.00 |
| Operating labor | 1.75/man hr. | $84.00 | $84.00 |
| Laboratory supervision | | $6.00 | $6.00 |
| Maintenance | | $75.00 | $75.00 |
| Total | | $277.60 | $619.60 |

## Transportation of Natural Gas

After the methane hydrate is removed from below the sea floor and preliminary processing has been done, a transportation selection has to be made. An initial assessment of cost between using a pipeline and a carrier are described in Tables 8 and 9. The values used in these tables for LNG carrier, assume 6 carriers, with a 130,000$m^3$ (or 7.09$Nm^3$, where 1$m^3$=613.6 $Nm^3$) capacity. It is important to note that an economic equivalence is achieved between 4000-6000 km of transportation distance. In the case of methane hydrate extraction at Hydrate Ridge, a site only 80km from the coast is being explored. Also, the cost of the pipeline is doubled when looking at placement on the sea floor, which is doubled again when the sea depth of the pipeline is over 500m. Due to the investment and operating costs of LNG carriers, only the use of pipelines will be considered for the scope of this project.

**Table 8: Initial capital investment for transportation of 130,000 $m^3$ over 1000km[Rojey et al., 1997].**

| Method | | US$ |
|---|---|---|
| Pipeline | Total | $0.9*10^9$ |
| LNG carrier | | |
| | Plant | $2.0*10^9$ |
| | Methane carrier | $1.2*10^9$ |
| | Regasification | $0.3*10^9$ |
| | Total | $3.5*10^9$ |

**Table 9: Annual costs for NG transportation per 1000 $Nm^3$ [Rojey et al., 1997].**

| Method | | US$ |
|---|---|---|
| Pipeline | Total | 20 |
| LNG carrier | | |
| | Plant | 55 |
| | Methane carrier(for 4000 nautical miles) | 35 |
| | Regasification | 11 |

| | |
|---|---|
| Total | 101 |

CNG through pipeline

In order to use pipelines for the transportation of compressed natural gas, it must undergo several steps. First, the sample is collected and processed before compression. After compression, the sample is fed to the pipeline where it will undergo several intermittent compression steps before arriving at the storage facility. An example of a commercial pipeline technology is the Yamburg-Uzhgorod pipeline that stretches over 4605 km [Rojey et al., 1997]. This pipeline, which has a flow of over 27 * $10^9$ $m^3$/year, has a pipe diameter of 56 inches (1.42m), and 38 compression stations. Each station has eight 25kW gas turbines.

Pipelines are classified by pipe diameter, materials, and schedule number. For this project, we will use the smallest standard diameter of pipeline, which is 8 inches. Stainless steel will be used, having a schedule number of 40 (40 is the standard schedule number used [Sinnott 1993]). The schedule number is classified by:

$$Schedule\# = P_s * 1000 \,/\, \sigma_s$$

Where $P_s$ = safe working pressure, bars
$\sigma_s$ = safe working stress, bars

A summary of the pipeline characteristics is listed in the table below. For the pipeline pressure, it is important to be less than the dew point pressure, but remain above the pressure for the reservoir.

**Table 10: Pipeline characteristics [Sinnott 1993].**

| | |
|---|---|
| Pipeline diameter | 8 inches |
| Pipeline length | 80km or 49.7 miles |
| Schedule number | 40 |
| Gas velocity | 15-30 m/s or 33.6-67.1 miles/hr |
| Pressure | 1.8-2.6 MPa |
| Maximum pressure drop | 0.02% of line pressure |

The velocity of the gas can be determined from the equation:

$$u = 4Q \,/\, \Pi\rho^2$$

Where u = velocity ($kg^2$/s)
Q = volume flow rate
ρ = density

In order to determine the pressure drop over a distance in the pipeline, use the formula below:

$$dW_f = f\left(\frac{\rho u^2}{2}\right)\left(\frac{dL}{D}\right)$$

Where L = line length
f = friction factor, typically close to 1 (laminar)
D = pipe diameter
$dW_f$ = pressure drop over distance traveled due to friction

As a rule of thumb, the cost of the pipeline is determined by:

Cost = D*A*miles of pipeline

Where D = diameter of pipeline
A= average cost of construction/ inch diameter mile

From this, the average cost in 1980 for 8 inch pipeline was $16,920/inch diameter mile, or a range of $6953-$24,125/ inch diameter mile [McAllister, 2002]. This cost comprises of four parts: right-of-way, materials, labor, and miscellaneous. The break down of these costs into percentage of total cost over a ten year period for 8 inch pipe is: right-of-way (2.8%), materials (37.2%), labor (49.2%), and miscellaneous (10.8%) [McAllister, 2002]. Using these calculations the approximate cost for the pipeline from Cascadia Ridge to the Oregon coastline are listed in the table below.

**Table 11: Estimated breakdown of costs for the pipeline.**

| | Cost range in US$ |
|---|---|
| Right-of-way | $77,406.36-$268,578.80 |
| Materials | $1,028398.76-$3,568,261.2 |
| Labor | $1,360,140.30-$4,719,313.20 |
| Misc. | $298,567.38-$1,035946.8 |
| Total | $2,764,512.80-$9,592,100 |

The overall cost for the use of pipelines from the Hydrate Ridge site will be closer to the maximum range figure of $9,592,100. This high cost can be attributed to the depth that the pipeline must be laid under water. Increased cost value can also be added to the pipeline when considering the fact that the pipeline is a permanent fixture and cannot be moved and reused once the production from the methane hydrate site is completed. Alternatives for transportation, such as a methane hydrate, may be considered if production from the Hydrate Ridge site is deemed feasible.

## FT Transportation by Tanker

When transporting the final Fischer-Tropsch product from the floating plant, very large crude carriers (VLCC) are the best option. Pipelines are not a flexible enough option for consideration. The debate is now, whether to rent or to buy a VLCC. When considering buying a VLCC there are many factors that go into the cost of a voyage, such as: speed, load, fuel quality, fuel cost, and weather conditions. A benefit of owning the vessel is the generated income from rental. As of January 1995, it cost $46,200/day to rent a vessel with 275,000-299,999 dead weight tons. These vessels have the dimensions listed in the table below.

**Table 12: Average specs for sea going VLCC [Golomer, 1996].**

| | Dimension |
|---|---|
| Draught | 20.9m |
| Length | 337.5m |
| Width | 55.2m |
| Dead weight | 280,786 tons |
| Million barrels | 2.10 |
| Speed | 15.6 knots |

When considering the purchase of a VLCC, we will look at the costs attributed to buying a single hull, 5-year-old vessel in good condition. Within these costs, insurance, labor, and maintenance must be considered. A break down of these costs is listed in the table below.

**Table 13: Operation expenses for the first 5 yrs of ownership [Golomer, 1996].**

| Market value of a 5yr old single hull in good condition | $65M |
|---|---|
| Average interest rate | 6% |
| Average payment period | 5 yrs |
| Hull and machine premium | $4000/day |
| Routine maintenance | $2000/day |
| Stores and lubes | $690/day |
| Administration | $1700/day |
| Crew | $2000/day |
| Total cost of ownership | $37,753/day |
| Rental cost | $46,200/day |

When the rental cost is compared to the ownership costs of a VLCC, it may seem that ownership is the best alternative. However, when considering the low production rates of the methane hydrate site, rental is the best option. The vessel would not be needed, except for several times a year. In order to make ownership profitable and worthwhile, the vessel would need to be at work for 350 days of the year. At this level, that would include the rental to outside businesses.

## Gas-To-Liquid Processes

The difficulties of NG transportation have limited its trading. An alternative way in NG utilization is to convert it into more valuable and easily transportable products. In the gas-to-liquid technology, natural gas is converted into a liquid product containing hydrocarbons and oxygenates. Three basic technologies exist, *i.e.* the gas-to-methanol technology, the gas-to-dimethylether technology (DME), and the gas-to-hydrocarbons technology, better known as the Fischer-Tropsch process. Gas-to-Methanol can provide a relatively low cost route process however; world methanol capacity is around 20% more than the world consumption. The elimination of MTBE in commercial fuels and opening of new methanol plants will make the situation of this technology even worse. Converting gas to generate higher alcohols and ethers is becoming more attractive because of their potential use in gasoline in the market [Rojey et al., 1997]. However, its use will be very limited until it can be proven as a transportation fuel. As a result the GTL process will focus only in the Fischer-Tropsch process to produce clean transportation fuels.

### Fischer Tropsch Process

Historically conventional FT catalyst and process technologies faced limitations due to the high capital cost of a GTL plant, limited premium product selectivity, inefficient reaction heat removal, catalyst deactivation, attrition, and inefficient catalyst recovery systems [Falbe, J., 1981, Anderson, R., 1984]. Recently, the growing availability of massive natural gas reserves, increasing environmental concern on transportation fuel, and gradual improvement in FT and related process technologies appear to be enhancing the economic prospects of FT processes. Diesel fuel is a superior fuel compared to gasoline. The volumetric calorific value for diesel fuel contributes to the fuel economy for diesel engine vehicles [Schobert, 1990]. The world has observed the economic benefits associated with using this superior fuel. As a result, Europe and Asia Pacific have gradually shifted from gasoline to diesel fuel. The world diesel consumption in 2005 is projected to be 40% greater than what it was in 2000 while that of the Asia Pacific is expected to be 90% more [Cakett, S. et al. 2002]. In the United States, the DOE has projected that the US demand of diesel will outpace the demand of gasoline in the next decade (48% and 43%, projected demand of diesel and gasoline respectively). At the same time the maximum allowable sulfur levels and other specifications for diesel are becoming particularly stringent. FT derived diesel has been

shown to exceed such specifications as shown in Table 14. These factors including the rapid increase of the crude oil prices that currently appear seems to be enhancing FT technology market.

**Table 14**: **Diesel specification for GTL with current and future regulations limit [adapted from Yakobson, 1999]**

| Properties | Current specifications | 2006 specifications | GTL |
|---|---|---|---|
| Sulfur (wt %) | <0.3 | <0.05 | ~0 |
| Aromatics (vol%) | <35 | <10 | ~0 |
| Cetane Index | >32 | >48 | 73 |

## Fischer-Tropsch Synthesis Technology

Three key process steps are generally required for FT based GTL diesel production. These steps are (1) Syngas generation with a minimum $H_2/CO$ ratio of just over 2:1; (2) FT synthesis of paraffin rich hydrocarbon liquids; and (3) Mild hydrocracking of the waxy paraffins to a diesel rich middle distillates fraction and fractionation of the distillate into the predominantly diesel product, along with byproducts kerosene, naphtha, heating oil, and LPG fuels.

Methane can be converted into synthesis gas by steam reforming or (catalytic) partial oxidation. Generally, the chemical process for steam reforming (1, 2, 3) and partial oxidation (4) of methane are described by the following equations:

$$CH_4 + H_2O \rightarrow 3H_2 + CO \qquad \Delta Hr^0 = 206\ kJ/mol \qquad (1)$$

$$CH_4 + CO_2 \rightarrow CO + 2H_2 \qquad \Delta Hr^0 = 247\ kJ/mol \qquad (2)$$

$$CO + H_2O \rightarrow CO_2 + H_2 \qquad \Delta Hr^0 = -41\ kJ/mol \qquad (3)$$

$$CH_4 + \tfrac{1}{2}\ O_2 \rightarrow CO + 2H_2 \qquad \Delta Hr^0 = -38\ kJ/mol \qquad (4)$$

Steam reforming involves the catalytic conversion of methane and steam to hydrogen and carbon oxides in the presence of a $Ni/Al_2O_3$ catalyst. This is done in a tubular furnace with heat recovery units [Rojey et al., 1997]. Water gas shift is another important reaction that occurs in the reformer. The reforming reaction is highly endothermic and is favored by high temperatures and low pressures. Higher pressures tend to lower the methane conversion. Typically temperature and pressure conditions are 850-940$^oC$ and under 3 MPa.

In steam reforming the side reaction of CO and hydrogen to produce water and carbon (reaction 5) must be controlled. If carbon formation occurs, it can poison the catalyst used in syn-gas generation. Excess steam is used to prevent coking in the reformer tubes. Steam-to-methane ($H_2O/CH_4$) ratio is usually in the range of 2:1-4:1 [Reyes et al., 2003], depending on the process conditions.

$$CO + H_2 \rightarrow C(s) + H_2O \qquad \Delta H = -131\ KJ/Mole \qquad (5)$$

Partial oxidation is carried out in a combustion chamber from 1200-1500$^oC$. A major side product of this reaction is carbon black. A typical partial oxidation reactor includes a burner with methane and oxygen, a heat recovery section, and a carbon black removal section [Rojey et al., 1997]. For both methods of reforming, it is necessary to control the $H_2/CO$ ratio in the gas output, because the favorable ratio for Fischer-Tropsch synthesis is between 2-2.5 [Rojey et al., 1997].

A newer process, introduced by Haldor Topsoe, is a combination of stream reforming and partial oxidation, termed autothermal reforming (ATR). Several researchers have reported that autothermal reforming (ATR) is the option of choice for large scale FT process. This is primarily attributed to the desired $H_2/CO$ ratio and the fact that there is a more favorable economy of scale for air separation units than for tubular reactors (steam methane reforming - SMR). Since this process is only viable for large scale FTS, the process will not be considered in this report. The basic FT reactor configurations that have been commercially applied to FTS are: (1) Tubular/Fixed bed reactor; (2) Fluidized bed reactor; and (3) Slurry bed reactor (also referred to as “slurry bubble column”).

Because of the highly exothermic reactions involved in FTS, a key factor in reactor design is the efficient removal of reaction heat and the maintenance of reasonably uniform temperature conditions. Among the factors influencing the choice of reactor configuration are production scale and whether the crude FT product is a gas or liquid phase under the reaction conditions [Falbe, J., 1981]. Other factors are capital and operation cost, product selectivity, catalyst attrition resistance and recovery. A comparison of the attributes, advantages, and disadvantages of these reactors are shown Table 15.

The slurry reactor has gained more attention recently. This technology will be applied in many plants in the world including Qatar's largest GTL plants. This reactor has simple construction, superior mixing of syngas with the catalyst, and smaller size for the same throughout [Anderson, R., 1984]. The FT reactors are operated at pressures ranging from 10-40 bar (145–580 psi). Upgrading is the last section of GTL plant. The upgrading usually means a combination of hydrotreating and hydrocracking in addition to product separation.

**Table 15: Evaluation of three common FT reactor systems [adapted from Guczi, L., 1991].**

| Attribute/Limitations | Fixed Bed | Fluid Bed | Slurry Bed |
|---|---|---|---|
| Relative capital cost | 208 | 100 | 46 |
| operation cost in $ million/year for 25,000 bbl/day | 14 | 6.72 | 0.76 |
| Thermal efficiency % | 85 | 66 | 91 |
| Temp control | fair | good | excellent |
| Product selectivity favored | heavy product and gasoline | high octane and gasoline | light olefins and waxy product |
| Product quality | good | fair | good |
| Activity maintenance | good | fair | fair-good |
| Ease of regeneration | poor | Very good | very good |
| • Reactor ideality | good | fair | fair |
| Stability | | | |
| • Flow | good | fair | fair |
| • Temp | fair | good | very good |

## Fischer-Tropsch Catalyst and Chemistry

### FT Chemistry

The Fischer-Tropsch reaction is the chemical heart in the gas-to-liquid technology. The basic steps of reaction are: (1) CO adsorption on the catalyst surface; (2) Chain initiation by CO dissociation followed by hydrogenation; (3) Chain growth (propagation) by insertion of additional CO molecules followed by hydrogenation; (4) chain termination; and (5) product desorption from the catalyst surface [Spath, P., L., and Dayton, D., C., 2003]

The FT generalized overall reaction stoichiometry can be written as follows:

$$CO + 2H_2 \rightarrow --CH_2-- + H_2O \qquad \Delta Hr^0 = -165 \text{ KJ/Mole} \qquad (6)$$

Understanding the mechanism of these polymerization reactions help in designing process, catalyst and set the optimum operation condition. For example, an essential characteristic of catalysts applied to FT diesel production is the ability to catalyze chain propagation versus chain termination steps. The carbon chain usually terminates by hydrogenation of the chain to produce a stable product. The specific selectivity for a particular hydrocarbon (long/short chain) and the overall product distribution

largely depend on catalyst type, temperature, and gas composition and are independent of chain length [Hensman, J. R., Ashley, M., 2004].

FT produces the following products: methane, alkanes and alkenes according to the following reactions:

| | | | | |
|---|---|---|---|---|
| $CO + 3H_2$ | → | $CH_4 + H_2O$ | Methanation | (7) |
| $nCO + (2n+1)H_2$ | → | $C_nH_{2n+2} + nH_2O$ | Paraffins | (8) |
| $nCO + 2nH_2$ | → | $C_nH_{2n} + nH_2O$ | Olefins | (9) |

Another competing reaction that becomes important in FTS is the Boudouard reaction:

| | | | | |
|---|---|---|---|---|
| $2CO$ | → | $C + CO_2$ | Boudouard | (10) |

The specific selectivity for a particular hydrocarbon and the overall product distribution may generally be described by a chain polymerization kinetics model involving the stepwise addition of one carbon to another on the growth chain [Guczi, L., 1991]. This model has been ascribed to Anderson, Schultz, and Flory and commonly referred to as the Anderson-Schultz-Flory (ASF) model. The ASF model can be presented mathematically be the following equation:

$$Wn/n = (1-\alpha)^2 \alpha^{(n-1)}$$

Where n = number of carbon atoms in the hydrocarbon molecule; Wn = weight fraction of product containing n carbon atoms; and α = chain growth propagation probability. This equation is graphically represented in Figure 7. It clearly displays the predicted distributions for several products and product ranges of particular interest.

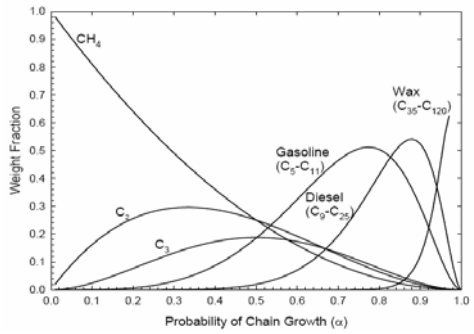


Higher value of α corresponds to increasingly heavier hydrocarbon selectivity as desired for FT diesel production, as determined by the choice of reaction conditions and catalyst. As clearly shown in the figure, for diesel production (diesel + wax) α has to be > 0.9. α can be increased by decreasing the temperature, decreasing $H_2/CO$, increasing reactor pressure. A typical net product distribution of FT appears to be roughly in the following ranges: (1) Diesel 35-45%; (2) Kerosene 25-35%; (3) Naphtha 20-30%; and (4) Heating Oil 0-5%.

**Figure 18: Chain growth probability (α) [Spath, P. et al. 2003].**

## Catalyst Development

FT catalyst systems involve some type of an inert support (i.e. alumina) with one or more active metals deposited on the support. Four metals are generally considered as ingredients for these catalysts - iron, cobalt, nickel, and ruthenium. Generally, the Ni catalyst is very active for hydrogenation reactions which leads to an enhanced methanation reaction at the cost of long chain hydrocarbon. As a result Ni catalysts are no longer used in methane based FT plants. Ruthenium has been applied in FT. It has been found to have high activity for FTS, however, due to its high cost; its use was limited only as a promoter [Guczi, L., 1991]. Depending on the types and quantities of FT products desired, either low temperature (200–240°C) or high temperature (300–350°C) synthesis is used with either an iron or cobalt catalyst. FTS temperatures are usually kept below 400°C to minimize $CH_4$ production (reaction 7) and to avoid coke formation (reaction 10).

Generally, cobalt catalysts are only used at low temperatures. This is because at higher temperatures, a significant amount of methane is produced. Low temperatures yield high molecular mass linear waxes (reaction 6) while high temperatures produce gasoline and low molecular weight olefins (reaction 7). If maximizing the gasoline product fraction, it is best to use an iron catalyst at a high

temperature in a fixed fluid bed reactor. If maximizing the diesel product fraction, a slurry reactor with a cobalt catalyst is the best choice. The most significant difference between Co and Fe catalyst is that the Co catalyst has low activity toward the water–gas-shift (WGS) reaction. WGS is undesired reaction due to the fact that more $CO_2$ will be release as well as the CO ratio decreases result on loss of final product yield. In addition, the WGS reaction consumes the generated heat in the FTS which otherwise can be utilized as valuable by-product.

## Optimum Utilization of NG from Hydrate Reservoir

Usually NG is brought to shore from the offshore location through pipelines, LNG carriers, or CNG carriers. The situation is more complicated and uneconomic when dealing with a small field of NG/methane hydrate such as the field assigned in this project. As a result, to deal with such fields new concept or design for utilizing NG that might enhance its economics is essential. We attempt to introduce a new concept of Fischer Tropsch Floating Plant (FTFP) to convert the NG into synthesis crude that can be easily transported by tanker.

NG Floating Plants or FTFP have not been used to date. However, several promising designs have been developed by oil and gas companies. Rentech (FT licenser) has announced that they are in the process of developing a conceptual FTFP with Worley and further studies are required for commercialization. Petroleum Geo-Services ASA and Syntroleum Corporation have agreed to develop and operate mobile marine plants, based on Syntroleum's GTL technology to convert natural gas from multiple offshore fields into hydrocarbon products.

There are several advantages of using FTFP for hydrate recovery and utilization. The main advantages that can justify our selection of FTFP are: (1) No fixed platform is required; (2) The mobility of the floating facilities would allow their use at multiple locations, thereby providing access to fields that are otherwise too small to justify permanent facilities; (3) Transportation of NG as liquid fuel (methanol or diesel) is the cheapest method for small field (< 13,000 bbl) [Imperial Venture Corp, 1998]; and (4) The valuable-by-product heat from FT can be integrated to generate steam that can be injected into the hydrate reservoir.

Ideally, FTFP has to be combined with other facilities to gain the advantages that are mentioned above. We suggest in this report that the floating plant contains production facilities (the equipment required for depressurizing & thermal processes), storage and offloading vessel in addition to FT plant.

Critical elements for the floating plant design are flexibility, energy integration, and compact design. As a result, our critical analysis will take into account these aspects. The slurry reactor, as mentioned above, has several advantages over other reactor types including the efficiency and compact design which make it the best fit for a floating plant. Synthesis gas generation unit has always been the reason for GTL process limitation due to the massive energy requirement and the high capitol cost (60% of total cost). Current reforming processes use either a large, heavy tubular steam reformer; or require large world-scale oxygen plants to allow the use of partial oxidation or autothermal reforming. Conventional reformers are large in size, massive in construction, and are highly capital intensive. Therefore, a significant issue for FTFP is to overcome the difficulties associated with reformers. Hensman and Ashley have designed a new steam reformer with excellent features such as simplicity and reliability, while at the same time improving energy efficiency [Hensman, J. R., Ashley, M., 2204]. Based on their design, a compact and efficient reformer is achievable which in turn will enhance the concept of FTFP. Their design of a compact reformer can produce a high quality synthesis gas with no nitrogen-based impurities of an air oxidation process, while not having the disadvantage of high expense for air separation in a catalytic oxidation process. The water moisture associated with methane from the hydrate reservoir can be utilized in the compact SMR and by-product water from FT can be recycled if required.

In summary, it is believed that the availability of a compact and flexible FTFP will improve process efficiency. The high value by-product heat can be integrated to increase the overall process efficiency. In addition, generating and injecting steam into the hydrate reservoir will open channeling,

increasing heat transfer and therefore increasing hydrate dissociation (increase gas production). If the field is hydrate limited, as expected in our case, then the ability to move the FTFP at the end of the production period would greatly enhance the process economics.

### Capital and operating costs

The rate of methane production is an important factor for Fischer Tropsch process design and hence the capital and production costs. For the purpose of preliminary economics evaluation, information from the literature has been reviewed and adapted to match with the purpose of this study. Recently, several studies done by Sasol and DOE indicated that the total capital cost of a GTL plant is in the order of about US$24,000/daily barrel [Anton C., 2001, Godwin A. 2002]. Further reduction of the total cost can be brought to about US$20,000/daily barrel by: (1) The economy of scale of larger capacity plants; (2) Improved process integration and optimization; and (3) Improved catalyst selectivity and activity as well as catalyst lifetime. Typical capital costs of a GTL plant can be broken down into the following: reforming (51%), FT synthesis (24%), product upgrading (13%), and power recovery (12%) [Anton C., 2001].

The capital cost associated with the syngas generation section is too high and a further dramatic cost reduction is essential to improve the marketing of Fischer Tropsch. If the compact steam reformer mentioned above is considered, this cost reduction might be achievable. More precisely, below is a preliminary cost evaluation for a floating plant that contains FTFP and other facilities, such as production, storage and offloading facilities. The evaluation is based on the following assumptions:

Diesel production rate = 1,330 bbl/d (methane input = 10 mmscfpd) {this amount might be achieved if heat is applied to the hydrate reservoir}.
Total capital cost includes FTP, production facility, storage facility, and offloading facility.
The cost does not include the cost of production rigs which usually can be leased.
Operation cost including catalyst, chemical, labor and feed (NG feed cost at $0.50/mmbtu)
Average diesel selling price = $50/bbl

**Cost Estimation**

| | |
|---|---|
| FT capital cost | = 24,000 * 1,330 = $31,920,000 |
| Production and storage facility cost | = $32,000,000 * 0.35 = $11,200,000 |
| Total capital cost | = $43,120,000 |
| Operation cost | = (11,200,000 + 31,920,000) * 0.18 = $7,761,600/year |
| Sales income | = 50 * 1,330 * 330 = $21,945,000 |

At this stage, the calculation does not account for tax and insurance, depreciation, discount cash flow, fluctuation, and administration and licenses fees. However, initial cost estimation calculations are promising and the FTFP might one day be the option of choice for remote and small hydrate fields.

## GTL Process Evaluation

The focus here will be on the process data including thermodynamic, kinetic, and design data to evaluate the GTL process through mass and energy balances.

## Thermodynamics and Kinetics Aspects

Steam reforming is based essentially on the oxidation of methane by water. The main reactions are as follow:

$CH_4 + H_2O \leftrightarrow 3H_2 + CO \quad \Delta Hr^0 = 206\ kJ/mol \quad (1)$

$CO + H_2O \leftrightarrow CO_2 + H_2 \quad \Delta Hr^0 = -41\ kJ/mol \quad (2)$

The reforming reaction is highly endothermic and is favored by high temperature and low pressure. The water gas shift reaction is slightly exothermic and is favored at low temperature. As a result, since temperature is too high for the CO equilibrium to shift towards $H_2$ production, $CO_2$ formation will be controlled. Data from [Chauvel, A., Lefebvre, G. 1989] shows the equilibrium concentration as a function of temperature and at 1 atm. The data can be presented graphically as shown in Figure 19. The figure shows that the reactor temperature significantly affects the equilibrium composition and the conversion. As the reactor temperature is raised from 600 to 950, the syngas conversion increases from around 65% up to over 99%. Hence, it can be assumed here, that the steam reformer at the desired operation conditions can achieve a 100 % conversion. High conversion of syngas is achieved which indicates that reforming

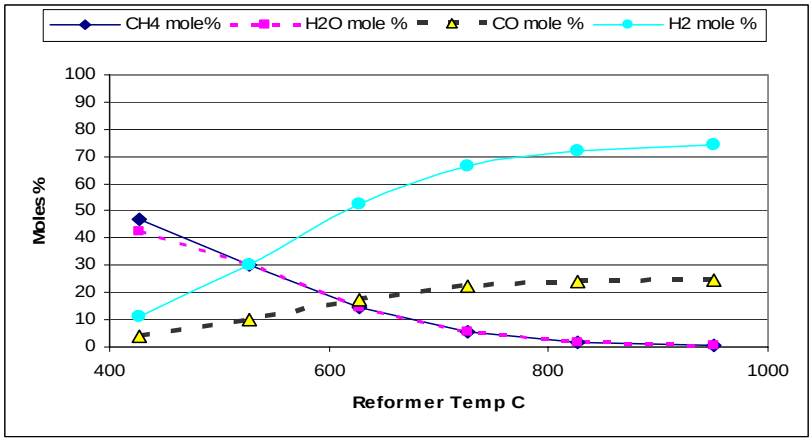


**Figure 19: Equilibrium concentration for syngas generation**

reactions for syngas generation are only slightly controlled by kinetics and thermodynamics. This of course was achieved at the expense of intensive energy consumption.

The FTS reaction is highly exothermic and accompanied by a reduction in the total number of molecules, it is therefore favored at low temperature and high pressure.

The Fischer-Tropsch synthesis is a complex network of parallel and series reactions involving different extents and determining altogether the overall catalyst performance. The whole synthesis reaction can be simplified as follow:

$nCO + (2n+1)H_2 \rightarrow C_nH_{2n+2} + nH_2O \quad \Delta Hr^0 = -165\ kJ/mol \quad (3)$

Optimal yields can only be achieved when the reactant CO and $H_2$, are introduced in the same ratio at which they are consumed by the reaction. Numerous research studies have been carried out to better understand the FTS reactions. Kinetics and thermodynamics as well as the reactions mechanism are too complicated and a full understanding of this mechanism is still lacking and disagreement still exists.

The thermodynamic probability of formation for products in a system of numerous parallel and secondary reactions that are in equilibrium is only possible when the simultaneous equilibria are calculated. However, this is not feasible with the FT system because of the theoretically unlimited number of reaction equations [Falbe, J., 1981].

The complex nature of the FT reaction and the large number of parameters (P, T, fresh gas composition, LHSV, mass and heat transfer, catalyst) contribute in the kinetics complexity and make the description of the kinetics difficult. Considering cobalt catalyst system, tens of equations are used for reaction rates determination.

| | | |
|---|---|---|
| $r = k\frac{P_{H^2}}{P_{CO}}$ | (1) | This equation used mostly in industrial sector [Falbe, J., 1981] |
| $r = k\frac{P_{CO}P_H}{P_{CO} + \alpha P_{H2O}}$ | (2) | This equation proposed by Anderson which includes water inhibition [Yang Jun, 2004]. |
| $r = k\frac{P_{CO}P_H}{P_{CO} + \alpha P_{CO2}}$ | (3) | This equation proposed by Ledakowicz and Deckwer which includes $CO_2$ inhibition, the WGS reaction will influence the reaction rate by altering the concentration of the reactants and products [Yang Jun, 2004]. |

In my opinion, the first rate equation is too simple to describe the rate of reaction. In addition, according to this equation, the rate of reaction is directly proportional to the square of hydrogen partial pressure and inversely proportional to the partial pressure of the carbon monoxide. Therefore, this equation cannot be reliable to express the rate of propagation of hydrocarbon, in which the carbon monoxide plays an important part to initiate and propagate this reaction. Hence, equation 2 and 3 are more realistic for overall kinetics estimation.

Since the study of the kinetics of such a complicated system is extremely difficult, no reliable data are available. Hence, the most convenient way to estimate reliable kinetics data is to conduct a pilot plant study taking into account all parameters that might affect the obtained data such as (P, T, fresh gas composition, LHSV, mass and heat transfer, catalyst).

## Process Design

The overall design of a process has the potential to affect the energy efficiency. Typically, a process is designed to make use of by-products and waste products in order to reduce process requirements. This, in turn, has the affect of increasing the overall energy efficiency. Usually, a good design takes into consideration the optimum process integration in terms of mass and energy.

For designing our FT process or more precisely the FTFP, we try to achieve the “optimum design”. This of course cannot be achieved with the limitations that we have. However, with some assumptions we will try to address the most efficient way for designing such a floating plant. For Example FTS is a highly exothermic process, an efficient way of utilizing this heat is to use a heat exchanger that can recover this heat. This heat in turn can be used to heat other units and if more heat is available then supply heat to increase hydrate dissociation will for sure improve the process efficiency. Similarly, the extra heat in the effluent stream for reforming is used to produce steam and reduce the number of boilers required.

The steam balance within the GTL plant is an important consideration because of the need to balance the sizable power demands of major steam users such as the steam reformer with substantial waste heat steam generation from major sources such as FT reactor and HCK effluents. Although a detailed optimization of the energy balances throughout the plant is beyond the scope of this report due to the limitation of resources and time, we have attempted to carryout energy balances and integrations for the main energy resources as well as the estimation of fuel and utilities requirements.

As mentioned in previous sections that one of the main advantage of FTFP is the ability to move the plant at the end of the production period. Consequently, the FTFP will not be limited for the current hydrate location. Ideally, the FTFP should be designed for utilizing daily NG throughout of around 40 mmscfd (5300 bbl/d oil equivalent). However, we have decided in this report to use a maximum

throughput of (5.32 E 5 mmscfd) which can be produced for four years. The proposed design parameters and bases are listed in Table 16.

## Material and Energy Evaluations

Material and energy balances for a complicated process such as FT process is usually carried out using especial simulation program. However, preliminary estimation can be achieved with acceptable reliability through simple hand calculations. Energy requirements of the process will be evaluated based on the design data mentioned previously. The main energy requirements in the process will be needed in the reformer and FTS. The reformer needs heat supplied for the endothermic reaction, while the FTS which is exothermic will require an efficient cooling system to remove the generated heat. Hence, heat integration for FT process is highly important to improve process efficiency. The simple block diagram (Figure 11) has been designed to achieve better efficiency. The excess hydrogen from steam reforming is efficiently utilized. Part of the excess hydrogen is used as the feed to the hydrocracking and the other part is used as fuel for the reformer.

**Table 16: Design bases and assumptions for the FT process.**

| Design Bases For FT plant | |
|---|---|
| Methane Throughput, scfd | 42,376,000 |
| Reactor System | |
| - Syngas generation | Steam reforming |
| - FT synthesis | Slurry Bed |
| - Hydrocracking | Trickle bed reactor |
| Syngas Generation | |
| - Catalyst type | Ni / silica alumina |
| - Exit temperature, C | 900 |
| - Exit pressure, bar | 25 |
| Syngas Molar Ratio | |
| - H2:CO | 3:1 |
| - H2:CO after H2 skimming | 2.1:1 |
| Fischer Tropsch Synthesis | |
| - Catalyst type | Co / silica alumina |
| - Exit temperature, C | 240 |
| - Exit pressure, bar | 20 |
| Hydrocracking | |
| - Catalyst type | Platinum / Zeolite |
| - Exit temperature, C | 385 |
| - Exit pressure, bar | 70 |

It is assumed that the desulfurized natural gas and steam are pretreated and delivered as a mixture at 110 C and 25 bar. The mixture is then preheated up to 500 C before it enters the steam reforming unit. The raw syngas exit the reformer at 900 C and 25 bar with an H2:CO ratio of about 3:1. The syngas undergoes cooling to about 240 C. The H2:CO ratio is reduced to 2.1:1 by skimming some hydrogen from syngas in the hydrogen-skimming unit. The syngas mixture with a H2:CO ratio of 2.1:1 enters the slurry FTS reactor. The FT reactions are highly exothermic; producing a heat of reaction of about (165 KJ/Mole) of CO reacted. The reaction conditions are maintained at 240 C and 20 bar in order to maximize the conversion of the syngas into desired higher molecular weights of hydrocarbon waxy products. The bottom product from the FTS reactor consists primarily of high molecular weight hydrocarbons. The heavy hydrocarbon is mixed with the skimmed hydrogen and sent to the hydrocracking unit. The

hydrocracker operates at a pressure of around 70 bar and a temperature of around 370 C. In this unit, the heavy hydrocarbons undergo mild hydrocracking to yield the desired diesel product.

Mass balance for the FT process is shown in Table 11. Based on our calculation, processing of 42,376,000 scfd of methane; produces 5830 bbl/d of diesel with 88 % yield of diesel. The mass balance was based on several assumptions: (1) complete decomposition of methane in the reformer to produce only 3:1 of $H_2$:CO as shown previously; (2) WGS reaction is controlled and avoided in the reformer and FTS; (3) No recycling streams are used to simplify the process; (4) Products from FTS are water and hydrocarbons; and (5) Hydrocarbons ranges from (C5-C13) are represented by $C_{10}H_{22}$, (C14-C19) are represented by $C_{16}H_{34}$, and (C19+) are represented by $C_{30}H_{62}$.

An energy balance is required to determine the energy requirements for FT process. The energy includes heating for reformer, cooling for FTS and HCK as major processes. In addition to the energy needed for the compressor to elevate the mixture (steam and methane) pressure from 1 bar to 25 bar. The conservation of energy relation for a chemically reacting steady-flow system can be expressed as:

$Q - W = H_P - H_R$

$H_P$ represents the enthalpy of products (the outlet streams) and $H_R$ represents the enthalpy of reactants (the inlet streams). Then $H_P$ and $H_R$ can be expressed in terms of enthalpies and mole numbers of their components as:

$$H_P = \sum N_P \left(h_f^0 + h_t + h^0\right)_P$$
$$H_R = \sum N_R \left(h_f^0 + h_t + h^0\right)_R$$

The subscript ° represents properties at a standard reference state of 25°C and 1 atm.

As mentioned above the syngas generation reaction is highly endothermic and hence extensive energy will be required to keep the reformer temp at 900 C. The excess hydrogen from the steam reforming can be used as clean fuel to generate heat for the reformer, according to the reaction below.

$2H_2 + O_2 \rightarrow 2H_2O \qquad \Delta Hr^0 = -484$ kJ/mol (3)

**Major Generated and Consumed Energy in the Process**

Reformer:

Heat required to raise reactant temperature + Heat consumed in system by endothermic reaction:

4,374,799 * [- 0.037 *(1173-773)] + [2,187,400*(- 206)] = <u>- 515,351 MJ/Hr</u>

Fischer Tropsch Synthesis:

Q = 2,194,895 * 165 = <u>362,158 MJ/Hr</u>

Hydrocracking:

Q = 25,025 * 50 = <u>1,251 MJ/Hr</u>

Compressor Energy Requirements:

Work (KJ/Kmol) = $Z1T1R\frac{n}{n-1}\left[\left(\frac{P2}{P1}\right)^{(n-1)/n} - 1\right]$, Take n = 1.5, and efficiency = 0.75

Work = 18.4 KJ/Mol * 4,374,799 Mol/Hr = 80,496,302 KJ/Hr /0.75 = <u>- 107,328 MJ/Hr</u>

Hydrogen Access Energy:

Q = 1952838 * 484 = 945,173,592 KJ/hr *0.75 = <u>708,880 MJ/Hr</u>

$Q_P$ = the balance Energy = [Energy Generated in the Plant] - [Energy Consumed by the Plant]

$Q_P$ = [1,072,364] – [622,605] = <u>449,610 MJ/Hr</u>

$Q_P$ = <u>124.9 MW</u>

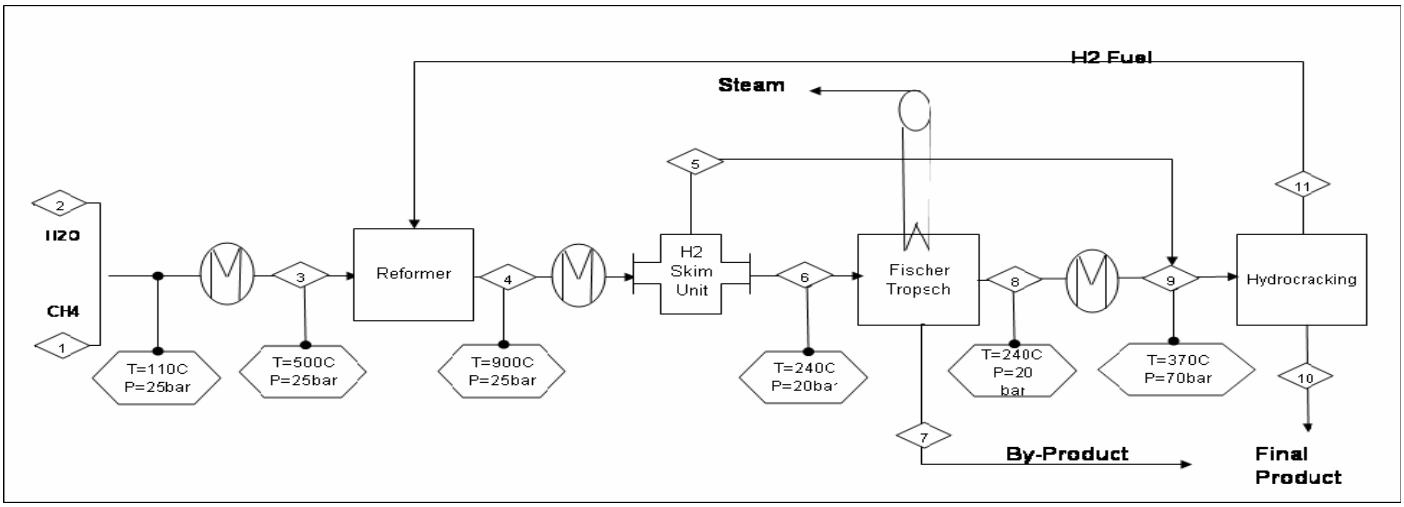


**Figure 20: Simplified block diagram for FT process.**

**Table 17: Mass Balance for Fischer Tropsch Process**

| | | NG feed 1 | Steam feed 2 | Reformer feed 3 | Reformer product 4 | Striped hydrogen 5 | FT feed 6 |
|---|---|---|---|---|---|---|---|
| | Mol. Wt | | | | | | |
| Temp (C) | | 110 | 110 | 500 | 900 | 240 | 240 |
| Pressure bar | | 25 | 25 | 25 | 25 | | 20 |
| | | | | - | | | |
| H2 | 2 | - | - | - | 12914.5 | 3937.4 | 8977.2 |
| CO | 28 | - | - | - | 61457.0 | - | 61457.0 |
| CH4 | 16 | 34998.4 | - | 34998.4 | - | - | - |
| *C5-C13 | 142 | - | - | - | - | - | - |
| ** C14-C19 | 228 | - | - | - | - | - | - |
| ***C19+ | 422 | - | - | - | - | - | - |
| H2O | 18 | - | 39373.2 | 39373.2 | - | - | - |
| **Total Kg/hr** | | 34998.4 | 39373.2 | 74371.6 | 74371.6 | 3937.4 | 70434.2 |

| | | FT by-product 7 | FT product 8 | HCK feed 9 | HCK product 10 | H2 Fuel 11 | |
|---|---|---|---|---|---|---|---|
| | Mol. Wt | | | | | | |
| Temp (C) | | | 240 | 370 | | | |
| Pressure bar | | | 20 | 70 | | | |
| H2 | 2 | - | - | 3937.4 | - | 3905.7 | - |
| CO | 28 | - | - | - | - | - | - |
| CH4 | 16 | - | - | - | - | - | - |
| *C5-C13 | 142 | 10250.1 | - | - | - | - | - |
| ** C14-C19 | 228 | 10250.1 | - | - | 10592.4 | - | - |
| ***C19+ | 422 | - | 10560.8 | 10560.8 | - | - | - |
| H2O | 18 | 39373.2 | - | - | - | - | - |
| **Total Kg/hr** | | 59873.5 | 10560.8 | 14498.1 | 10592.4 | 3905.7 | |

| ***Inlet Stream*** | | ***Outlet Streams*** | |
|---|---|---|---|
| CH4 | 34998 | CH4 | 0 |
| Steam | 39373 | H2 | 3905.7 |
| | | H2O | 39373.2 |
| | | C5-C13 | 10250.1 |
| | | C14-C19 | 20842.6 |
| Total (Kg/hr) | 74371.6 | | 74371.6 |

| ***Diesel*** | ***Production Rate*** |
|---|---|
| C5-C13 | 10250.1 |
| C14-C19 | 20842.6 |
| Total Diesel (kg/hr) | 31092.72 |
| Total Diesel (bbl/d) | 5830.2 |

## Energy Recovery and Heat Integration

Process streams at high pressure and/or temperature; contain energy that can be usefully recovered. In the situation of FTFP, the energy cost is too high and therefore recovering techniques is valuable. The most common energy recovery technique is to utilize the heat in a high temperature process stream to heat a colder stream and at the same time cooling the hot stream (heat integration). Since the FTFP is designed to be compact, heating loss will be minimized and hence the cost of recovery will be greatly reduced. Process integration can lead to a substantial reduction in the energy requirement. One of the most successful techniques for heat integration is "pinch technology".

From the block diagram, some streams are to be heated and other to be cooled. We will construct the pinch network to estimate the net load needed or available in the process.
For detail calculations, please see the appendix A

Table 18 shows the heat load for the streams that need to be exchanged to reach to the target temperature. It is very clear that stream number 4 in the block diagram that exits from the reformer has a huge amount of energy that will be sufficient to provide heat for most of other streams to reach to their target temperature.

**Table 18: Heat load for numbers of streams in the plant**

| Stream number | Type | Heat Capacity KW/C | Source Temp | Target Temp | Heat Load KW |
|---|---|---|---|---|---|
| 4 | Hot | 35 | 900 | 240 | 23379 |
| 10 | Hot | 5.9 | 370 | 50 | 1883 |
| 3 | Cold | 24 | 110 | 500 | 9573 |
| 8 | Cold | 5.7 | 240 | 370 | 744 |

Table 14 and 15 shows the required calculation to estimate the pinch where the minimum temperature difference between the streams of 20 ºC. The pinch occurs where the heat transferred is zero, that is at interval number 5, at temp = 230 ºC as shown in table 15.

**Table 19: Algorithm for heat integration**

| Stream number | Actual Temperature | | Interval Temperature | |
|---|---|---|---|---|
| | Source Temp | Target Temp | Source Temp | Target Temp |
| 4 | 900 | 240 | 890 | 230 |
| 10 | 370 | 50 | 360 | 40 |
| 3 | 110 | 500 | 120 | 510 |
| 8 | 240 | 370 | 250 | 380 |

**Table 20: Algorithm for heat integration, indicating the pinch zone**

| Interval | Interval Temp C | ΔT | ΣCPc*ΣCPh | ΔH (KW) | Cascade | |
|---|---|---|---|---|---|---|
| | 890 | | | | 0 | -16527 |
| 1 | 510 | 380 | -35 | -13461 | 13461 | -3066 |
| 2 | 380 | 130 | -11 | -1414 | 14874 | -1653 |
| 3 | 360 | 20 | -5 | -103 | 14978 | -1550 |
| 4 | 250 | 110 | -11 | -1214 | 16192 | -335 |
| 5 | 230 | 20 | -17 | -335 | 16527 | 0 |
| 6 | 120 | 110 | 19 | 2053 | 14474 | -2053 |
| 7 | 40 | 80 | -6 | -471 | 14945 | -1582 |

The pinch occurs at interval number 5, at 230 ºC. So at the pinch the hot streams will be at 240 ºC and the cold streams will be at 220 ºC. Figure 21 shows the integration network. The network indicates that with better integration, no hot utility will be required. Cold streams (stream 3 & 8) will absorb the required heat to reach to their target temperature by integration with hot streams (stream 4 & 10). The number of utilities in the plant reduced to only two individual utilities as shown in the network. Note that without heat integration, four individual utilities will be the minimum number of utilities required as shown in the process block diagram. In addition, 14.9 MW (16.527 MW – 1.582 MW) is available in site that can be utilized for other purposes such as generating steam for hydrate dissociation.

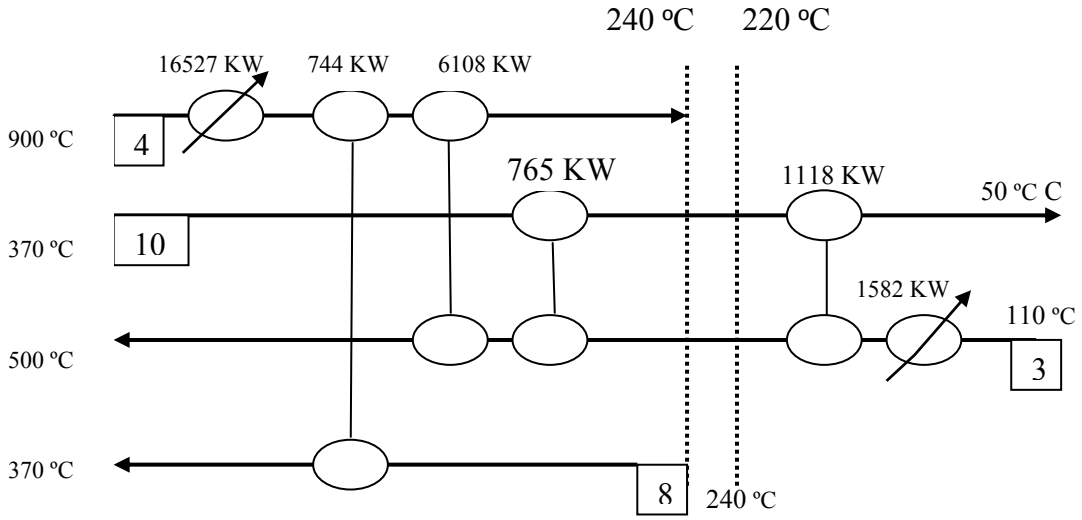


**Figure 21: Heat integration network for the GTL plant**

The overall energy recovery in the FTFP is the sum of the energy released from different unit operations, heat released from hydrogen combustion, and the heat recovered by heat integration.

Numerically, the total energy available in site is (124.9 + 14.9) = 139.8 MW. This valuable energy can be utilized as addition energy to supply heat for the hydrate reservoir. Ideally, heat integration between down and upstream will enhance and improve the overall efficiency of the project.

Energy Efficiency

The energy efficiency is the amount of the useful energy extracted from a system divided by the amount of energy put into the system in order to recover the energy. Usually the input energy into the system is the total energy of the supplementary fuel, external electricity, and the energy stored in the process feed. In the case of FTFP no additional fuel will be provided and all of the required fuel will be extracted from the by-product hydrogen. If electricity will be required, an internal turbine can be constructed from the steam generated in the process. The heat integration network and the energy balance evaluation shows that the energy released in the process exceeds the required energy for the process. Hence, the FTFP process efficiency can be measured from the total amount of energy content of diesel product, divided by the total amount of energy content of input methane.

Methane input to the process = 42,376,054 $ft^3$/day

The useful energy can be expressed in Btu; one $ft^3$ of methane releases 1,000Btu

Based on the material balance; 42,376,054 $ft^3$/day of methane produces 5830 bbl/d of diesel. The amount of Btu in one gallon of diesel is 139,000 Btu.

$$\text{Process Efficiency} = \frac{5{,}830 \times 42 \times 139{,}000}{42{,}376{,}054 \times 1000} \times 100 = 80\ \%$$

## Global Carbon Cycle and Potential Effects of Methane Hydrates to Environment

The importance of methane hydrates in the global carbon cycle is that methane hydrates are one of the major global carbon reservoirs containing %0.014 of the total amount with 10000 giga tons of carbon. This makes methane hydrates a potential energy source because the amount of carbon in this promising source is more than double that of conventional fossil fuels which contain 4200 giga ton carbon.(http://bama.ua.edu/~bsc5561/BSC456_556_Spring2003_BiogeochemicalCyclesCarbonPart1_Slides.pdf)

The major carbon-containing component in the atmosphere is carbon dioxide with the concentration increasing at a considerable rate of 0.35% per year (Kvenvolden, 1988). Methane is another carbon containing component whose concentration is also increasing at a rate of 1-2% per year. Why this increase is important is that it causes an increasing retention of radiant heat by the atmosphere which is also known as greenhouse effect and a higher equilibrium temperature for the Earth. Methane may be short-lived relative to carbon dioxide, with an atmospheric lifespan of 12 years; however it is 23 times more effective as a green house gas, on a weight basis. Although methane is one the greenhouse gases in the atmosphere, according to Kvenvolden, huge amounts of methane from dissociated methane hydrate never reaches the atmosphere due to oxidation. Therefore, methane produced from methane hydrate may not affect global climate change. (Kvenvolden 1999) On the other hand, methane hydrates could potentially pose a risk to both the environment through increased greenhouse gas emissions and also to deep sea drilling rigs situated above shifting hydrate deposits. Hydrates create a potential natural hazard threat associated with sealer instability and the release of methane to the oceans and atmosphere; disturbing hydrate deposits during drilling could pose a threat to drilling rigs.
(http://www.agiweb.org/gap/legis106/hydrate52599.html)

Hazards arise because gas hydrates are only quasi-stable; if the temperature is increased at a fixed pressure or the pressure decreased at fixed temperature, or both temperatures increased and pressure decreased, it is easy to pass out of the stability regime of hydrates. Destabilization of the hydrates with an uncontrolled release of large volumes of methane is a significant hazard.

(http://www.ncseonline.org/NLE/CRSreports/energy/eng46.cfm?&CFID=17303960&CFTOKEN=21072543)

### Effects of enhanced recovery

The depressurization production model considered under this research shows that an insufficient volume of hydrate can be dissociated, as methane production from hydrates is 3 orders of magnitude less than that of free gas. A substantial volume of methane has been documented to exist, however without significant contribution from methane hydrates the production scheme can not be considered viable. Hydrate reserves at Hydrate Ridge have shown to be insufficient however this research provides insight to alternative future site investigations.

Within this research project it was assumed that production of free gas below the hydrates would have no adverse effects in terms of slope stability. Also, since hydrate dissociation was minimal it was assumed that overpressures would be insignificant. However, with enhanced dissociation, such as thermal injection, a viable approach for hydrate recovery may be possible. As more aggressive approaches are undertaken, environmental considerations become more relevant with the need for slope stability analyses and worst-case scenarios to be considered.

The mechanisms controlling gas hydrate-induced sea floor subsidence and landslides are not well known, but these processes may release large volumes of methane to the Earth's oceans and atmosphere. Due to hydrates occurring at shallow depths they may be vulnerable to perturbations and subsequently release, possibly affecting global climate (Glasby, 2003).

As discussed, even a catastrophic release of methane hydrates at a particular site would not be likely to deliver 100% of the hydrated methane to the atmosphere. However assuming a worst-case scenario for the Nankai Trough which represents the largest known reserve estimates of methane hydrates, a catastrophic release would only amass 0.38% of the total annual methane emissions (Figure 22). The effects of such severe local methane concentrations would of course need to be assessed prior to drilling operations; however it seems unlikely that global climatology would be affected.

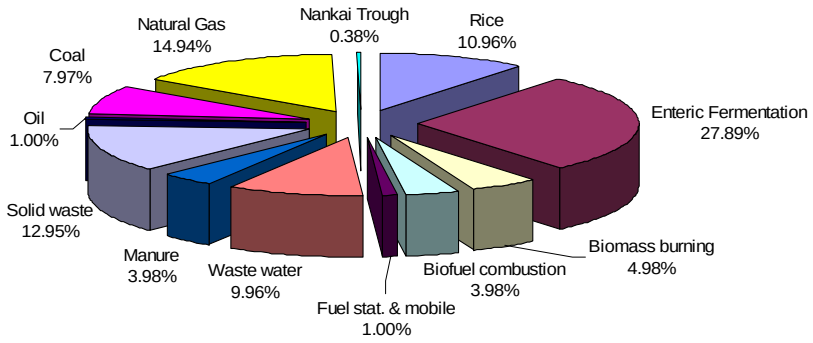


**Figure 22: Methane emission sources with the inclusion of the Nankai Trough methane hydrates [adapted from the Environmental Protection Agency]**

## Economic Evaluation

Two different methods are selected to convert methane hydrate to a salable product in the market: First selection is using a *Fischer Tropsch Floating Plant* for diesel production and the second one is using *Pipeline Construction* for natural gas production. The first option is used for utilizing gas which could not be brought to the market due to unavailable pipelines or no local use. Such situations may be used for remote production areas from the market like deep offshore waters. Second is the efficient and effective

way to transport natural gas from producing regions to consumption regions because a pipeline requires an extensive and elaborate transportation system.

To evaluate cash flow diagram for these two alternatives, cost elements of each step to produce commercial products are calculated.

Table 21 shows the cost distribution of a well in the drilling process. Costs are in the units of $ millions and those steps are the most important ones required for cost evaluation. Drilling costs and platform costs are needed for both of the alternative processing methods and in Table 22; they are listed as Field Development.

**Table 21: Cost Distribution of a Well for Drilling Process**

| **Drilling-Cost Distribution of a Well** | **Footnote for reference** | **Cost($MM)** |
|---|---|---|
| Wellhead | Dawe 2000 | 0.1 |
| Flow line and Surface Equipment. | Dawe 2000 | 0.16 |
| Casing and Down hole Equipment. | Dawe 2000 | 1.465 |
| Drilling Contractor | Dawe 2000 | 2.06 |
| Directional Drilling | Dawe 2000 | 0.32 |
| Logging/Testing/Perforating | Dawe 2000 | 0.6 |
| Mud Processing/Chemicals | Dawe 2000 | 0.86 |
| Cementing | Dawe 2000 | 0.29 |
| Bits | Dawe 2000 | 0.28 |
| Av. cost of 3D seismic program conducted in Atlantic Canada | http://www.capp.ca/raw.asp?x=1&dt=PDF&dn=74365 | 15 |
| Drill Rig ($350,000–$450,000/day) | 552hr=23day | 9.2 |
| Supply Vessel ($15,000 -$30,000/day) | 400day | 6 |
| Well Evaluation - $10-$15 Million/well | http://www.capp.ca/raw.asp?x=1&dt=PDF&dn=74365 | 10 |
| **Drilling Cost - $30-$60 Million/well** | http://www.capp.ca/raw.asp?x=1&dt=PDF&dn=74365 | **46.335** |
| **Platform Cost ($MM)** | Dawe 2000 | **180** |

In Table 21, operation of drill rigs required 552 hrs and it is calculated as 23 days with 100% efficiency. Also, supply vessels will be used continually during the 400 days of production time.

**Table 22: Cost Elements for the Options: FTFP and Pipeline Construction**

| **Items for FTFP** | FTFP Pay Back Time for Diesel Production $MM | Pipeline Pay Back Time for NG Production $MM | **Items for Pipeline Cons.** |
|---|---|---|---|
| Field Development | -226.335 | -226.335 | Field Development |
| | | -9.592 | Pipeline Construction |
| Fischer Tropsch Plant | -139.920 | | |
| w/ Depreciation | -13.992 | | |
| Floating Plant/Storage/Offloading | -105 | | |
| Sweetening Cost (Chp 5) | -0.1 | -0.1 | Sweetening Cost (Chp 5) |
| Total Capital Cost | -485 | -236 | Total Capital Cost |
| Operation Cost/Total Time | -24 | -7.447 | Operation Cost/Total Time |
| Diesel Sell $/bbl | 60 | 0.005 | NG Sell $/ft3 |
| Total Operation Days | 400 | 400 | Total Operation Days |
| Diesel Production/Day | 5830 | 42376054 | NG Production/Day |
| **Income** :Diesel Sell/Total Days | 139.920 | 89.837 | **Income:** NG Sell/Total Days |

**Table 23: Cumulative Cash Flow of FTFP and Pipeline Construction wrt Time**

| Time (years) | Cumulative cash flow ($MM) [FTFP] | Cumulative cash flow ($MM) PipeLine |
|---|---|---|
| 0 | 0 | 0 |
| 1 | -485 | -236 |
| 2 | -369 | -154 |
| 3 | -254 | -71 |
| 4 | -138 | 11 |
| 5 | -22 | 94 |
| 6 | 94 | 176 |
| 7 | 210 | 258 |
| 8 | 326 | 341 |
| 9 | 442 | 423 |
| 10 | 558 | 505 |

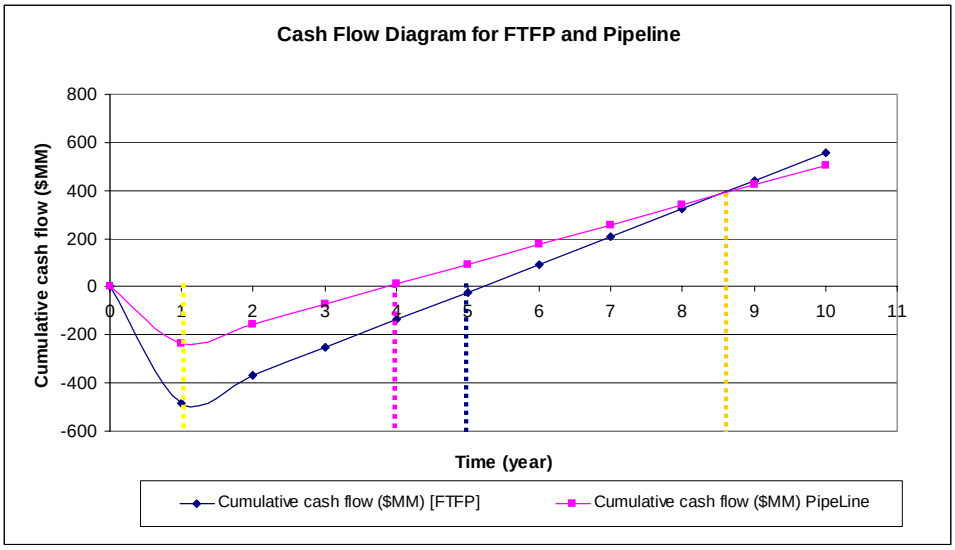


**Figure 23: Cash Flow Diagram for FTFP and Pipeline**

Figure 23 predicts the cash flow for FTFP and pipeline depending on the number of years of sustained production rates.

There are four different steps in offshore oil and gas processing, basically *exploration*, searching for petroleum using geophysical techniques, *development*, drilling wells and laying pipelines, engineering, fabrication/construction, *production*, transportation to market and *abandonment*, completion of project. For the sake of simplicity in the economic analysis of drilling some of those steps are not evaluated. In the economic analysis of diesel and natural gas production from methane hydrates the cost of drilling, FT floating plant construction, sweetening, pipeline construction costs are determined. Natural gas production cost analysis is done using field development (cost of platform and drilling), cost of pipeline construction and sweetening as capital cost and diesel production cost analysis contains FT plant and its depreciation cost, floating plant, storage and offloading as well as field development and sweetening again as capital cost.

In Figure 23, it is seen the maximum capital cost is during building the plant until production starts. Those costs are $\$485*10^6$ and $\$236*10^6$ for FTFP and Pipeline constructions, respectively. After one year the plant starts to produce pay back time. At the end of the 400 days and during this operation time it is clearly seen that both options are invisible and the deficits for Pipeline and FTFP options are $ 154 and $ 369 millions, respectively. Figure 16 also shows that pay back time of pipeline option can be achieved after 3 years operation while it will required one more year for FTFP. Assumably, if the amount of hydrate is four times of the current amount, the pipeline will be the alternative; however if the amount of hydrate available can be assumed to be 6 times of the current one, FTFP will be the option.

## Conclusions

Hydrate reservoirs have proven to be economically feasible through depressurization schemes. Therefore Pismaniye Aslanlari has considered the use of a passive and simplistic depressurization model to produce natural gas from offshore methane hydrates and available free gas at Southern Hydrate Ridge. The model is developed around the exploitation of an exisiting pressure gradient. Theoretically the reservoir pressure delivers natural gas from the free gas zone, while the associated pressure drop dissociates the overlying methane hydrates. An economic analysis was used to determine the feasibility

of production based on a single well drilled to a depth of 125m. The total recovery from the well before abandonment was found to be $5 * 10^8$ scm which is around 50% of the estimated reserves of site 1249 and 1250. The market price of both the products are calculated as -

Using the pipeline transportation technique -
Total cost of producing methane from the Oregon site, transporting and processing = $ 243.4 * 106
To breakeven the production costs, the market price of the natural gas product from Pismaniye Aslanlari should be set at = $ 243.4 * $10^6$ / 5 * $10^8$ scm = $ 0.486 / scm
This value is 257 % higher than the current market selling price of methane = $ 5.36 / 1000 scf = $ 0.189 / scm

Using the GTL technique -
Total cost of producing methane from the Oregon site and producing diesel from it through GTL process = $ 509 * $10^6$
Amount of diesel produced from 5* $10^8$ scm methane = 2332000 bbl
To breakeven the production costs, the market price from Pismaniye Aslanlari should be set at = $ 218.267 / bbl

This value is 364 % higher than the current market selling price of diesel = $ 60 / bbl

This shows that for the quantities of product we have and the time frame considered here, selling it as natural gas would be better than selling it as diesel. But the main advantage to using the GTL technique would be that the overall energy recovery from the FTFP provides an additional 139.8 MW and this energy can be utilized as additional energy to supply heat for the hydrate zone. Ideally heat integration between the down and upstream will enhance and improve the overall efficiency of the system.

To make Pismaniye's natural gas product competitive in the current market, we should have had one of the following different in the reservoir conditions -
1) At 11 MPa, $\Phi = 0.2$, $S_{wi} = 0.15$, Recoverable amount = 1.3* $10^9$ scm i.e. minimum volume in the reservoir should be = 2.6 * $10^9$ scm.

2) At 511 MPa, 5 * $10^8$ scm, $\Phi = 0.2$, $S_{wi} = 0.15$

**Table 24: Reservoir yield variation with saturation and porosity**

| $\Phi$ (%) | $S_{wi}$ (%) | Yield from reservoir ($m^3$) |
|---|---|---|
| 0.1 | 0.1 | 5.36E+08 |
| 0.1 | 0.9 | 4.50E+07 |
| 0.9 | 0.1 | 5.63E+08 |
| 0.9 | 0.9 | 5.06E+08 |

It was observed that as the porosity was increased, the amount recovered increased, and as water saturation was increased, the yield reduced. This agrees with the findings of (Khatnair 2002). Inspite of considering the minimum saturation and maximum porosity conditions, the yield is not sufficient to match the 1.3* $10^9$ scm requirement.

Had the amount of hydrate dissociated in the reservoir been larger, the main considerations for choosing one technique over the other is the payback time of each. The pipeline option can be achieved after three years of operation while it will require four years for the same for the GTL technique. Assuming at the amount of hydrate is quadrupled, the pipeline would be the choice of option. However if

the amount of hydrate available can be assumed to be six times of the current amount, the GTL will be the best choice.

---

As shown, the low permeabilities of 8E-15$m^2$ in clayey sediments is one of the biggest limiting step in recovery processes. Therefore an increase in permeability is required for production schemes located in silt or clay deposits. Lithostatic forces near the seafloor are such that any injection into the pore structure will disrupt or fracture the sediment fabric. Fracturing of the sediment may actually produce desirable results. With the addition of sand in the GTL-heated brine, the fractures will remain in tact leaving a medium with increased surface area contact and recovery potential.

**Future Consideration**

Thermal injection coupled with a depressurization model may lead to a viable approach for hydrate recovery. The Gas-to-Liquids process developed in coordination with the optimal recovery of methane hydrates yields an excess of 140,000 kW. To overcome the stability of hydrates, thermal injection will aid depressurization bringing hydrate recovery closer to reality. This quantity of heat is theoretically in excess of the amount of energy required to dissociate the entire hydrate reserve at the 300m x 500m site. However it should be noted that this calculation is incomplete due to the poor understanding of local heat sinks at this site.

The first go/no-go consideration to be addressed is the reserve estimates. Secondly, the concentration and density of the resource needs to be taken into account. Additionally, the location of hydrate reserves plays an integral part in the feasibility of recovery schemes. The first consideration is depth; significant and concentrated hydrate resources are typically shallow lying. Fractures which may continue to the seafloor can act as conduits for methane, producing structural accumulations. These accumulations generally have high methane saturations since overburden pressures decrease with proximity to the seafloor. The second consideration is the proximity to an in-place infrastructure. This research has shown that transportation costs associated with remote reserves may likely prove cost prohibitive. Several potentially viable hydrate reserves are outlined in Table 25.

**Table 25: Profiles of potentially viable hydrate reserves**

| Region | Area, $km^2$ | Depth, m | Resource, $m^3$ | Resource Density $m^3/km^2$ | Gas Hydrate Concentration, vol% |
|---|---|---|---|---|---|
| Hydrate Ridge | 375 | 700-1000 | 9E9 | 2.4E7 | Avg. 1-8, up to 40 |
| NW Gulf of Mexico | 23,000 | 440-2500 | 8-11E12 | 3.5-4.8E8 | Avg. 20-30 up to 100 |
| Haakon Mosby | 1.8 | 1250 | 3E8 | 1.66E8 | up to 25 |
| Blake Ridge | 26,000 | 1000-4000 | 2.8E13 | 1.1E9 | Avg. 2 up to 14 |
| Nankai Trough | 32,000 | 700-3500 | 6E13 | 1.9E9 | Avg. 10 up to 30 |

## References

Ahmadi, G. and D. H. Smith (2004). "Numerical solution for natural gas porduction from methane hydrate dissociation." J. Petroleum Science & Engr **41**(4): 269-285.

Baker, R. (1994). A Primer of Oil Well Drilling - A basic text of Oil & Gas Drilling. Austin, Petroleum Extension Service.

Baker, R. (1998). A Primer of Offshore Operations. Austin, Petroleum Extension Service.

Chauvel, A., Lefebvre, G., (1989). Petrochemical Processes; Synthesis-Gas Derivatives and Major Hydrocarbons. Paris, Editions Technip.

Clennel, M. B., M. Hovland, J. S. Booth, P. Henry and W. J. Winters (1999). "Formation of natural gas hydrates in marine sediments 1. Conceptual model of gas hydrate growth conditioned by host sediment properties." Journal of Geophysical Research-Soled Earth **104**(B10): 22985-23003.

Collett, T. S. (1998). "Hydrates contain vast store of world gas resources." Oil and Gas Journal **96**(19): 90-95.

DOI (2004). Offshore Minerals Management.

EIA (2004). Costs and Indices for Domestic Oil and Gas Field Equipment and Production Operations: 1987 through 2003. Washington D.C, Energy Information Administration, US-DOE.

EPA (2004). Region 10: The Pacific Northwest.

Giavarini, C. and F. Maccioni (2004). "Self-preservation at low pressures of methane hydrates with various gas contents." Ind. Eng. Chem. Res. **43**(20): 6616-6621.

Goel N., W. M., Shah S., (2001). "Analytical modeling of gas recovery from in situ hydrates dissociation." J Petroleum Science & Eng. **29**: 115 - 127.

Golomer, O. (1996). The Market and Economics of Large OIl Tankers. London, Oxford Instituite for Energy Studies.

Holder, G. D. and P. F. Angert (1982). "Simulation of gas production from a reservoir containing both gas hydrates and free natural gas." SPE.

Hong H., P.-D. M., Bishnoi P.R., (2003). "Analytical modelling of gas production from hydrates in porous media." J Canadian Petroleum Technology **42**(11): 45 - 55.

Kamath V.A., M. P. N., Sira J.H., Patil S. L., (1991). "Experimental study of brine injection and depressurization methods for dissociation of gas hydrates." SPE Formation Evaluation(SPE 19810).

Kastner, M., K. A. Kvenvolden, M. J. Whiticar, A. Camerlenghi and T. D. Lorenson (1995). Relation between pore fluid chemistry and gas hydrates associated with bottom-simulating reflectors at the Cascadia Margin, sites 889 and 892. Ocean Drilling Program, Scientific Results.

Khataniar S., Kamath V.A., Omenihu S.D., Patil S. L., Dandekar A. Y.; **(2002)** " Modelling and Economic Analysis of gas production from hydrates by depressurization model" Canadian J Che Eng., 80, 135-142.

Kim H. C., B. P. R., Heidemann R. A., and Rizvi S. S. H., (1987). "Kinetics of methane hydrate decomposition." Chem. Eng. Science **42**: 1645 - 1653.

Kohl, A. and F. Riesenfeld (1985). Gas Purification. Houston, TX, Gulf Publishing Co.

Kvenvolden, K. A., (1995) 'A review of the Geochemistry of Methane in natural Gas Hydrate' Organic Geochemistry, Vol. 23, No:11/12 pp. 997-1008,

Kvenvolden, K. A. (1988) 'Methane Hydrate-A Major Reservoir of Carbon In the Shallow Geosphere', Chemical Geology, 71, 41-51

Lederhos J.P., Long J.P., Sum A., Christiansen R.L. and Sloan E.D. Jr, (1996) 'Effective Kinetic Inhibitors For Natural Gas Hydrates', Chem. Eng. Science, 51, No:8, pp 1221-1229

Link, D.D. et al. (2003) 'Formation and Dissociation Studies for Optimizing the Uptake of Methane by Methane Hydrates' Fluid Phase Equilibria, 211, 1-10

MacKay, M. E., R. D. Jarrard, G. K. Westbrook and R. D. Hyndman (1994). "Origin of bottom-simulating reflectors- Geophysical evidence from the Cascadia accretionary prism." Geology **22**(5): 459-462.

Makagon, Y. F. (1997). Hydrates of Hydrocarbons, PennWell Books.
McAllister, E. W., Ed. (2002). Pipeline Rules of Thumb Handbook. Boston, Gulf Professional Publishing.

McGuire P.L. (1982). "Recovery of gas from hydrate deposits using conventional technology." SPE/DOE(SPE/DOE 10832).

Milkov, A. V. a. S. R. (2002). "Economic geology of offshore gas hydrate accumulations and provinces." Marine and Petrochemical Geology **19**(1): 1-11.

Moridis G. J., C. T. S. (2003). "Strategies for gas production from hydrate accumulations under various geological and reservoir conditions." Proc. TOUGH Symposium 2003: 1 - 8.

Moridis G. J., C. T. S., Dallimore S. R., Satoh T., Hancock S., Weatherill B. (2004). "Numerical studies of gas production from several $CH_4$ hydrate zones at the Mallik site, Mackenzie Delta, Canada." J Petroleum Science & Eng. **43**: 219-238.

Pooladi-Darvish M. (2004). "Gas production from hydrate reservoirs and its modeling." SPE(SPE 86827).

Reyes, S. C., J. H. Sinfelt and J. S. Feeley (2003). "Evolution of processes for synthesis gas production: recent developments in an old technology." Ind. Eng. Chem. Res. **42**: 1588-1597.

Rojey, A., C. Jaffret, S. Cornot-Gandolphe, B. Durand, S. Jullian and M. Valais (1997). Natural Gas: Production, Processing, Transport. Paris, Editions Technip.

Schobert, H. H. (1990). The Chemistry of Hydrocarbon Fuels. Boston, MA, Butterworths.

Sinnott, R. K. (1993) Coulson & Richardson's Chemical Engineering: Chemical Engineering Design, Butterworth-Heinemann.

Sira, J.H., Patil, S.L., Kamath, V.A., (1990) "Study of Hydate Dissociation by Methanol and Glycol Injection" SPE 20770

Sloan E. Dendy, Jr. Sloan, E. Dendy, (1994) 'Clathrate hydrates of natural gases'

Sloan E. D. Jr (2003). "Fundamental principles and applications of natural gas hydrates." Nature **426**: 353 - 359.

Tan, B. B., J. T. Germaine, P. B. Flemings, D. Goldberg and A. Janik (2003). "Consolidatin characteristics of hydrate saturated sediments from ODP Site 1244, Hydrate Ridge, Cascadia Continental Margin." Eos. Trans. AGU.

Travert, A., C. Dujardin, F. Mauge, S. Cristol, J. F. Paul, E. Payen and D. Bougeard (2001). "Parallel between infrared characterization and ab initio calculations of CO adsorption on sulphided Mo catalysts." Catalysis Today **70**(1-3): 255-269.

Trehu, A. M., G. Bohrman, F. R. Rack and M. E. Torres (2003). Leg 204 Summary, Ocean Drilling Program.

Trehu, A. M. and E. R. Fleuh (2001). "Estimating the thickness of the free gas zone beneath Hydrate Ridge, Oregon continental margin, from seismic velocities and attenuation." Journal of Geophysical Research-Soled Earth **106**(B2): 2035-2045.

Trehu, A. M., P. E. Long, M. E. Torres, G. Bohrman, F. R. Rack, T. S. Collett, D. Goldberg and A. V. Milkov (2004). "Three-dimensional distribution of gas hydrate beneath southern Hydrate Ridge." Earth and Planetary Science Letters **222**: 845-862.

Tsypkin G.G. (2000). "Mathematical models of gas hydrates dissociation in porous media." **912**: 428 - 436.

Wolman, D. (2003). Gas goes solid, MIT's technology review.

Yang, J., (2004). A review of kinetics for Fischer-Tropsch synthesis. Chemical Journal on Internet, USA.

http://www.gasprocessors.com/GlobalDocuments/E1Nov_01.pdf

http://www.marad.dot.gov/MARAD_statistics/PDF/Offshore%20Drill%20Rig.pdf

http://www.capp.ca/raw.asp?x=1&dt=PDF&dn=74365

Kvenvolden, K.A. (1999), 'Potential Effects of Gas Hydrate on Human Welfare', Proc. Natl. Acad. Sci.,

Vol. 96, pp 3420-3426.

Kvenvolden, K.A. (1988), "Methane Hydrate-A Major Reservoir of Carbon in the Shallow Geosphere?",

Chemical Geology, 71, pp 41-51

E. Dendy Sloan, Jr. Sloan, E. Dendy 'Clathrate hydrates of natural gases', 1944

Sira J.H., Patil S.L. 'Study of Hydrate Dissociation by Methanol and Glycol Injection' 1990, Society of Petroleum Engineers

Grauls D., (2001) "Gas Hydrates: importance and applications in petroleum exploration", Marine and Petroleum Geology 18, pp 519-523

Glasby, G.P., (2003) "Potential Impact on Climate of the Exploitation of Methane Hydrate Deposits Offshore", Marine and Petroleum Geology 20, pp 163-175

Dawe Richard A., "Modern Petroleum Technology" Volume 1 Upstream, John Wiley and Sons Ltd. , 2000, 6th Ed.

http://www.wrh.noaa.gov/climate/index.php?wfo=pqr